Electronic Supplementary Material (ESI) for Green Chemistry. This journal is © The Royal Society of Chemistry

One-step Selective Cleavage of C_α–C_β Bond in Lignin Models by Bifunctional Pyridinium Photocatalyst via PCET Process

Cai-Hui Rao, Hao-Ran Wei, Xiao-Li Miao, Meng-Ze Jia, Xin-Rong Yao, Xiao-Yan Zheng* and Jie Zhang*

MOE Key Laboratory of Cluster Science, Beijing Key Laboratory of Photoelectronic /Electrophotonic Conversion Materials, School of Chemistry and Chemical Engineering, Beijing Institute of Technology, Beijing 102488, P. R. China.
*E-mail for corresponding author: xiaoyanzheng@bit.edu.cn; zhangjie68@bit.edu.cn;

Table of Contents

Section 1. Experimental details

1.1 Materials and instrumentation

All chemicals are obtained from commercial sources and were of GR/AR grade unless otherwise noted. Photocatalytic reactions are carried out by using multichannel photochemical reaction systems SSSTECH-LAL1CV1.0 from Shanghai 3S Technology Co., Ltd. Infrared spectra (KBr pellets) are obtained on a Nicolet iS10 FT-IR spectrometer. The UV-Vis absorption spectra are measured with a Shimadzu UV3600 spectrometer. Fluorescence emission spectra are measured with a Hitachi F-7000 spectrometer. NMR spectra are measured with a Bruker Bio Spin AVANCE III spectrometer. Electron spin resonance measurements are recorded using a JES-FA200 spectrometer. The gas chromatography analyses are performed on Shimadzu GC-2014 C with the FID detector equipped with an Rtx-5 capillary column. HRMS was performed on Q Exactive HF-X LC-MS, Chromatograph: U3000nano UPLC, Vanquish UPLC; Ion Spray: ESI, nanoESI, APCI, APPI. The cyclic voltammetry measurements are conducted on a CHI660E electrochemical workstation (Chenhua Instrument, Shanghai, China).

1.2 Synthetic procedures

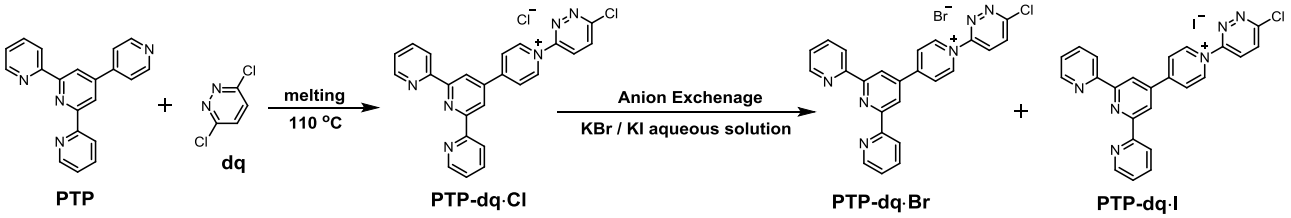

PTP-dq·Cl: A mixture of 3,6-dichloropyridazine (4.0 g, 26.8 mmol) and 4'-(4-pyridyl)-2,2':6',2"-terpyridine (PTP) (1.0 g, 3.2 mmol) was added into in a 50 mL flask and stirred in the molten state at 110 °C for 15 h. After that, 30 mL acetonitrile was added into the reaction flask, and then the mixture was ultrasonically treated for 10 minutes. The precipitate was collected by filtration and washed three times with acetonitrile. The crude product was recrystallized in distilled water to give PTP-dq·Cl as a yellow powder (1.1 g, yield: 76 %). The catalyst PTP-dq·Br and PTP-dq·I was obtained by anion exchange. ^{1}H NMR (400 MHz, CD_3OD) δ [ppm]: 9.82 (d, J = 7.2 Hz, 2H), 9.04 (s, 2H), 8.95 (d, J = 7.2 Hz, 2H), 8.76 (d, J = 4.0 Hz, 2H), 8.72 (d, J = 8.0 Hz, 2H), 8.62 (d, J = 9.2 Hz, 1H), 8.38 (d, J = 9.2 Hz, 1H), 8.06 (t, 2H), 8.05 (t, 2H). ^{13}C NMR (101 MHz, DMSO-d_6) δ 159.03, 157.06, 156.73, 156.66, 154.68, 149.99, 144.57, 143.85, 138.25, 133.03, 127.56, 126.38, 125.59, 121.76, 119.56. HRMS (ESI$^+$) m/z: [PTP-dq]$^+$ calcd for $C_{24}H_{16}ClN_6$: 423.11195; found: 423.11198.

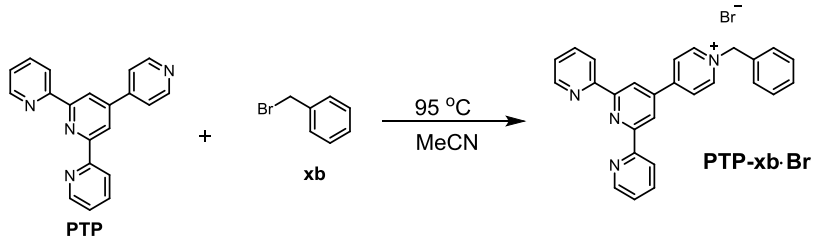

PTP-xb·Br: A mixture of (bromomethyl)benzene (0.7 g, 3.8 mmol) and 4'-(4-pyridyl)-2,2':6',2"-terpyridine (1.0 g, 3.2 mmol) was dissolved in 10 mL of acetonitrile and then stirred at 95 °C for 8 h. The crude product was collected by filtration after the reaction mixture was cooled to room temperature. The product was washed with acetonitrile for three times, and then dried in an air oven at 80 °C to give PTP-xb·Br as a yellow powder (1.2 g, 80%). ^{1}H NMR (400 MHz, DMSO-d_6) δ [ppm]: 9.32 (d, J = 7.2 Hz, 2H), 8.85 (s, 2H), 8.74 (m, 4H), 8.65 (d, J = 8.0 Hz, 2H), 8.05 (t, 2H), 7.59 (m, 2H), 7.54 (t, 2H), 7.46 (m, 2H), 5.94 (s, 2H). ^{13}C NMR (101 MHz, DMSO-d_6) δ 156.84, 154.64,

153.74, 149.90, 145.77, 144.30, 138.23, 134.61, 129.95, 129.78, 129.27, 126.83, 125.52, 121.71, 119.29, 63.52. HRMS (ESI$^+$) m/z: [PTP-xb]$^+$ calcd for $C_{27}H_{21}N_4$: 401.1761; found: 401.1758.

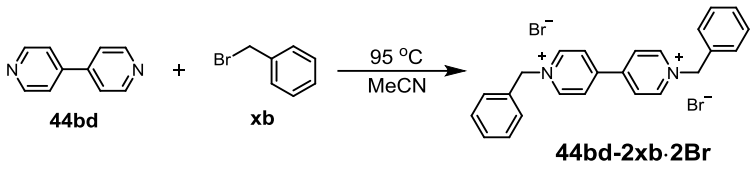

44bd xb 44bd-2xb·2Br

44bd-2xb·2Br: A mixture of (bromomethyl)benzene (2.7 g, 16.0 mmol) and 4,4'-bipyridine (44bd) (1.0 g, 6.4 mmol) was dissolved in 100 mL of acetonitrile and then stirred at 95 °C for 2 h. The crude product was collected by filtration, and washed with acetonitrile for three times, and then dried in an air oven at 80 °C to give 44bd-2xb·2Br as a yellow powder (2.2 g, 70%).^{1}H NMR (400 MHz, D_2O) δ [ppm]: 9.17 (d, J = 6.0 Hz, 2H), 8.54 (d, J = 5.6 Hz, 2H), 7.55 (s, 5H), 5.95 (s, 2H). ^{13}C NMR (101 MHz, D_2O) δ 150.28, 145.50, 132.20, 130.16, 129.66, 129.29, 127.09, 64.82. HRMS (ESI$^+$) m/z: [44bd-xb]$^{2+}$ calcd for $C_{24}H_{22}N_2$: 169.0886; found: 169.0883.

1.3 Photoreaction methods

For the photocatalytic reaction, in general, a mixture of 0.01 mmol of photocatalyst, 0.2 mmol of the substrate and 5 mL of the solvent is placed in a reaction hall. The photoreaction is initiated at room temperature under an air atmosphere. The electric power of the photoreactor is set at 6W in all reactions. The light intensity is 373.53, 370.23, 336.39, and 222.27 (mW/cm^2) for 365 nm, 395nm, 410nm, and white light source respectively. Products are confirmed by GC-MS spectra and compared with standard samples. The conversion of the substrate, the selectivity of the product, and the percentage content of the compounds are calculated by GC analyses. Other control experiments are carried out under the same reaction conditions except for changes in the substrate and irradiation wavelength, as well as exposure to an N_2 or O_2 atmosphere.

1.4 Electrochemical measurements

The cyclic voltammetry (CV) measurements are performed in acetonitrile containing 0.4 mM of photocatalyst by using the three-electrode system with the glassy carbon electrode (GCE) as the working electrode, the saturated calomel electrode (SCE) as the reference electrode, and the platinum electrode as the auxiliary electrode. The electrolyte is tetrabutylammonium hexafluorophosphate (1.9 mM). The excited state energy of the first singlet excited state S1 and excited state reduction potential (E^*_{red}) are calculated by [1]:

$$E_{0,0} = hc/\lambda$$

$$E_{red}^* (cat^*/cat^{\bullet-}) = E_{red} (cat/cat^{\bullet-}) + E_{0,0}$$

Note: The excited state energy is often named with the subscript "0,0", which refers to the transition between the lowest energy vibrational state (v = 0) of S1 to v = 0 of S0, which can be estimated at the midpoint between absorption and emission maxima.[1]

[1] N. A. Romero, D. A. Nicewicz, *Chem. Rev.* 2016, **116**, 10075.

1.5 Density functional theory calculations

All the density functional theory (DFT) calculations were performed with Gaussian 16 software.[1] The DFT method was employed using the (U)B3LYP functional.[2] The 6-31G* basis sets [3] were used for the atom in geometry optimizations using the polarizable continuum model (PCM) [4] with acetonitrile. Frequency analyses were carried out to confirm each structure being a minimum (no imaginary frequency) or a transition state (only one imaginary frequency). Furthermore, intrinsic reaction coordinate (IRC) calculations were carried out to confirm that

transition state structures connect to the appropriate reactants and products. The single-point energy calculations were carried out using the 6-311+G(d,p) basis set to provide better energy correction. Furthermore, the spin-orbital coupling constant (SOC) are performed using the ORCA package [5] at the B3LYP/6-31G* level.

[1] M. J. Frisch, G. W. Trucks, H. B. Schlegel, G. E. Scuseria, M. A. Robb, J. R. Cheeseman, G. Scalmani, V. Barone, G. A. Petersson, H. Nakatsuji, X. Li, M. Caricato, A. V. Marenich, J. Bloino, B. G. Janesko, R. Gomperts, B. Mennucci, H. P. Hratchian, J. V. Ortiz, A. F. Izmaylov, J. L. Sonnenberg, Williams, F. Ding, F. Lipparini, F. Egidi, J. Goings, B. Peng, A. Petrone, T. Henderson, D. Ranasinghe, V. G. Zakrzewski, J. Gao, N. Rega, G. Zheng, W. Liang, M. Hada, M. Ehara, K. Toyota, R. Fukuda, J. Hasegawa, M. Ishida, T. Nakajima, Y. Honda, O. Kitao, H. Nakai, T. Vreven, K. Throssell, J. A. Montgomery Jr., J. E. Peralta, F. Ogliaro, M. J. Bearpark, J. J. Heyd, E. N. Brothers, K. N. Kudin, V. N. Staroverov, T. A. Keith, R. Kobayashi, J. Normand, K. Raghavachari, A. P. Rendell, J. C. Burant, S. S. Iyengar, J. Tomasi, M. Cossi, J. M. Millam, M. Klene, C. Adamo, R. Cammi, J. W. Ochterski, R. L. Martin, K. Morokuma, O. Farkas, J. B. Foresman and D. J. Fox, *Gaussian 16, Revision A. 03*, Gaussian Inc., Wallingford, CT, 2016

[2] S. Grimme, J. Antony, S. Ehrlich and H. Krieg, *J. Chem. Phys.* 2010, **132**, 154104.

[3] W. J. Hehre, R. Ditchfield and J. A. Pople, *J. Chem. Phys.* 1972, **56**, 2257.

[4] J. Tomasi, B. Mennucci and R. Cammi, *Chem. Rev.* 2005, **105**, 2999.

[5] F. Neese, F. Wennmohs, U. Becker and C. Riplinger, , *J.Chem. Phys.* 2020, **152**, 224108.

Section 2. Data of Tables

Table S1. Control experiment of the oxidation cleavage of C-C bonds in **1**. [a]

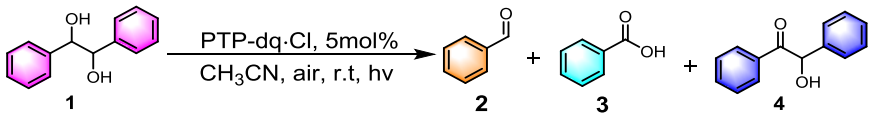

1 2 3 4

Entry	Photocatalyst	Conv. (%)	Yield of **2** (%)	Yield of **3** (%)	Yield of **4** (%)	Note
1	no catalyst	–	–	–	–	in air
2	PTP-dq·Cl	–	–	–	–	in dark
3	PTP-dq·Cl	96	78	14	5	in air
4	PTP-dq·Cl	98	77	18	2	in O_2
5	PTP-dq·Cl	3	2	–	1	in N_2
6	PTP	2	–	–	2	in air
7	dq	–	–	–	–	in air
8	44bd	–	–	–	–	in air

[a] Standard reaction condition: 0.2 mmol of 1,2-diphenylethane-1,2-diol (**1**) and 5 mol% of photocatalyst in 5 mL of acetonitrile at room temperature under an air atmosphere by irradiation with 410 nm light source for 2 h. PTP: 4'-(pyridin-4-yl)-2,2':6',2"-terpyridine, dq: 3,6-dichloropyridazine. 44bd: 4,4'-bipyridine.

Table S2. Comparison of performances between our work and some typical reports of β-O-4 conversion.

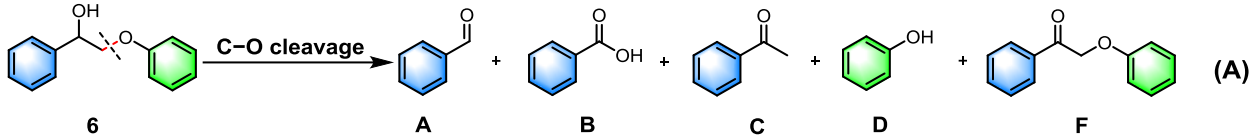

Entry	Reaction conditions	Dosage (**6**)	Conv. (%)	Product distribution or yield (%)				
				A	**B**	**C**	**D**	**F**
1[1]	CdS-Ag_2S, air, N_2, blue-LED, 3 h.	0.05 mmol	99			95	91	4
2[2]	NaOH, H_2O, N_2, 110 °C, 12h.	0.4 mmol	95			79	76	
3[3]	Rh, NaOH, H_2O, N_2, 110 °C, 18 h.	0.2 mmol	99			86	89	8
4[4]	Re_2O_7, p-xylene, 140 °C, 4h	1.23 mmol	99				81	
5[5]	Ni/CdS, KOH, CH_3CH, blue hv 3 h.	0.1 mmol	99			99	99	
6[6]	1. Pd(OAc), DMSO, air, 65 °C, 18 h.	0.4 mmol	99					97
	2. [Ir], Pr_2NET, HCO_2H, MeCN, blue, 32 h.	0.7 mmol	99			94	92	
7[7]	Ni/MgAlO-C, CH_3OH, H_2 (1 MPa), 200 °C, 6 h.	0.2 mmol	99			99	99	
8[8]	CdS NPs, CH_3CN, N_2, visible light	0.1 mmol	99			91	93	8
9[9]	$ZnIn_2S_4$, CH_3CN, 42 °C, Argon, hv 455 nm, 4 h.	0.1 mmol	99			83	90	9
10[10]	1. $NaNO_2$, DDQ, NHPI, CH_3CN, O_2, 80 °C, 2 h.	0.15 mmol	99					95
	2. NiMo sulfide, methanol, H_2 (1.0 MPa), 180 °C, 6 h.	0.2 mmol	95			89	72	
11[11]	1. $VOSO_4$, TEMPO, O_2 (0.4 MPa), CH_3CN, 100 °C, 12 h.	0.5 mmol	99					82
	2. $Cu(OAc)_2$-bpy, MeOH, O_2 (0.4 MPa), 80 °C, 2 h	0.2 mmol	92	10	50		43	
12[12]	1. Pd/$ZnIn_2S_4$, TiO_2, NaOAc, EtOH, O_2, hv-455nm, 28 h.	0.1 mmol	99					90
	2. TiO_2, NaOAc, EtOH, N_2, hv-365nm 5h.	0.1 mmol	94			76	94	
13[13]	Pd/CeO_2	0.6 mmol	68			33	40	
14[14]	HCOOH/H_2O, HCOONa, 110 °C, 12 h	0.2 mmol	99			96	87	
15[15]	[Ir], DIPEA, HCO_2H, CH3OH, hv, 18 h.	0.4 mmol	99			90	92	

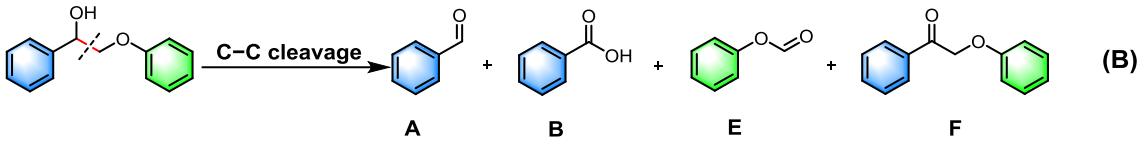

Entry	Reaction conditions	Dosage (**6**)	Conv. (%)	Product distribution or yield (%)			
				A	**B**	**E**	**F**
1[16]	Ir, base, PhSH, bule LED, r.t, 1.2V, 12 h.	0.1 mmol	99	95		93	
2[17]	mpg-C_3N_4, CH_3CN, O_2 (1 atm), hv-455 nm, 10 h.	0.05 mmol	96	51	21	30	7
3[18]	Ru/CeO_2, $CuCl_2$, H_2O, 200 °C, Ar, 6 h.	0.2 mmol	90		34	73	
4[19]	[V], CH_3CN, O_2, white LED, 24 h.	0.03 mmol	76	68		51	
5[20]	$Cu(OAc)_2$, ligand, KOH, DMSO, O_2 (0.4 MPa), 100 °C, 2 h.	0.2 mmol	99		76		
This work	Pyridinium, air, r.t, hv-365nm, 3 h	0.2 mmol	99	25	24	35	2
	Pyridinium, air, r.t, hv-365nm, 5 h	0.2 mmol	99	6	45	38	1

Note: The content of products was calculated by the distribution percentage in this work.

Reference

[1] H. Yoo, M. Lee, S. Lee, J. Lee, S. Cho, H. Lee, H. G. Cha, H. S. Kim, *ACS catal.* **2020**, *10*, 8465.

[2] Y. Liu, C. Li, W. Miao, W. Tang, D. Xue, J. Xiao, T. Zhang, C. Wang, *Green Chem.* **2020**, *22*, 33.

[3] Y. Liu, C. Li, W. Miao, W. Tang, D. Xue, C. Li, B. Zhang, J. Xiao, A. Wang, T. Zhang, C. Wang, *ACS Catal.* **2019**, *9*, 4441.

[4] B. J. Hofmann, R. G. Harms, S. P. Schwaminger, R. M. Reich, F. E. Kühn, *J. Catal.* **2019**, *373*, 190.

[5] G. Han, T. Yan, W. Zhang, Y. C. Zhang, D. Y. Lee, Z. Cao, Y. Sun, *ACS Catal.* **2019**, *9*, 11341.

[6] G. Magallanes, M. D. Kärkäs, I. Bosque, S. Lee, S. Maldonado, C. R. J. Stephenson, *ACS Catal.* **2019**, *9*, 2252.

[7] M. Wang, X. Zhang, H. Li, J. Lu, M. Liu, F. Wang, *ACS catal.* **2018**, *8*, 1614.

[8] X. Wu, X. Fan, S. Xie, J. Lin, J. Cheng, Q. Zhang, L. Chen, Y. Wang, *Nat. Catal.* **2018**, *1*, 772.

[9] N. Luo, M. Wang, H. Li, J. Zhang, T. Hou, H. Chen, X. Zhang, J. Lu, F. Wang, *ACS Catal.* **2017**, *7*, 4571.

[10] C. Zhang, H. Li, J. Lu, X. Zhang, K. E. MacArthur, M. Heggen, F. Wang, *ACS Catal.* **2017**, *7*, 3419.

[11] M. Wang, J. Lu, X. Zhang, L. Li, H. Li, N. Luo, F. Wang, *ACS Catal.* **2016**, *6*, 6086.

[12] N. Luo, M. Wang, H. Li, J. Zhang, H. Liu, F. Wang, *ACS Catal.* **2016**, *6*, 7716.

[13] W. Deng, H. Zhang, X. Wu, R. Li, Q. Zhang, Y. Wang, *Green Chem.* **2015**, *17*, 5009.

[14] A. Rahimi, A. Ulbrich, J. J. Coon, S. S. Stahl, *Nature* **2014**, *515*, 249.

[15] J. D. Nguyen, B. S. Matsuura, C. R. J. Stephenson, *J. Am. Chem. Soc.* **2014**, *136*, 1218.

[16] Y. Wang, Y. Liu, J. He, Y. Zhang, *Sci. Bull.* **2019**, *64*, 1658.

[17] H. Liu, H. Li, J. Lu, S. Zeng, M. Wang, N. Luo, S. Xu, F. Wang, *ACS Catal.* **2018**, *8*, 4761.

[18] M. Wang, M. Liu, H. Li, Z. Zhao, X. Zhang, F. Wang, *ACS Catal.* **2018**, *8*, 6837.

[19] S. Gazi, M. Đokić, A. M. P. Moeljadi, R. Ganguly, H. Hirao, H. S. Soo, *ACS Catal.* **2017**, *7*, 4682.

[20] M. Wang, J. Lu, L. Li, H. Li, H. Liu, F. Wang, *J. Catal.* **2017**, *348*, 160.

Table S3. Bond distance change when N1 of the pyridazine unit reacts with **6**.

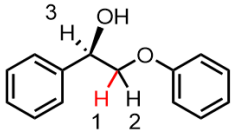

	Bond distance change when N1 reacts with 6 (Å)			
	C−H1	C−H2	C−H3	C−C
Catalyst	1.097	1.097	1.101	1.532
Ts-ini	1.094	1.093	1.099	1.531
Ts	1.293	1.095	1.098	1.540
Ts-Pro	3.064	1.088	1.100	1.498

Section 3. Characterization of catalyst structure

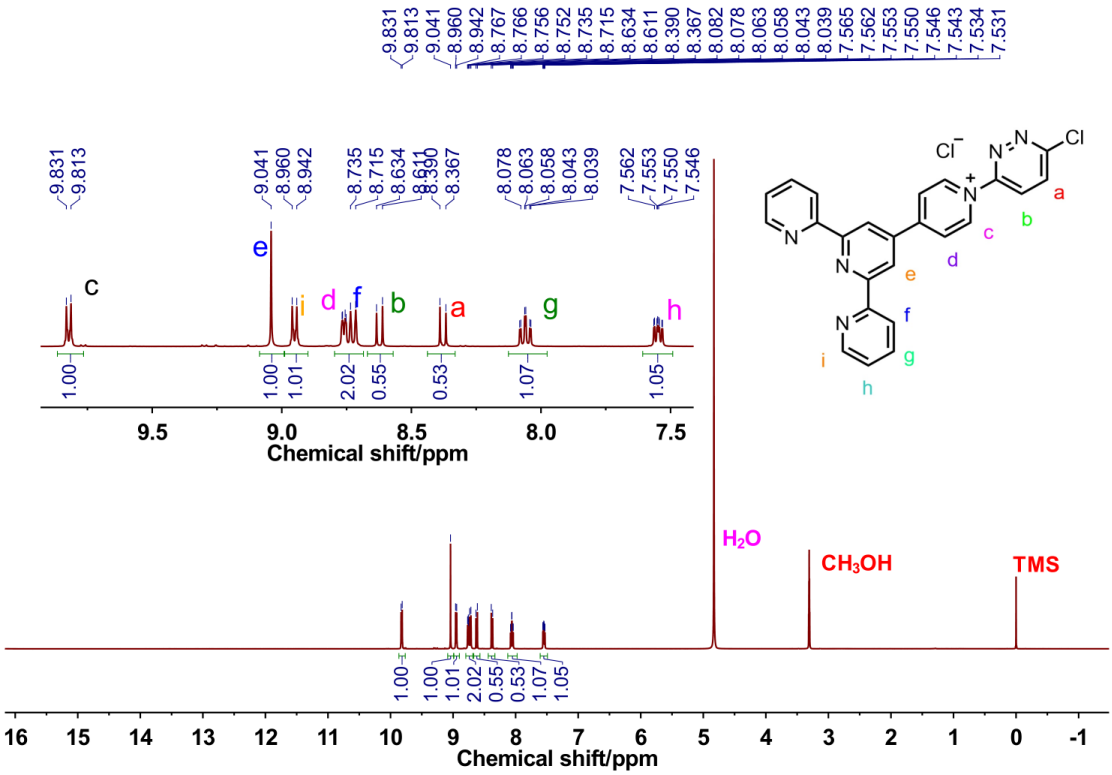

Figure S1. ^{1}H NMR (400 MHz) spectrum of PTP-dq·Cl in CD_3OD.

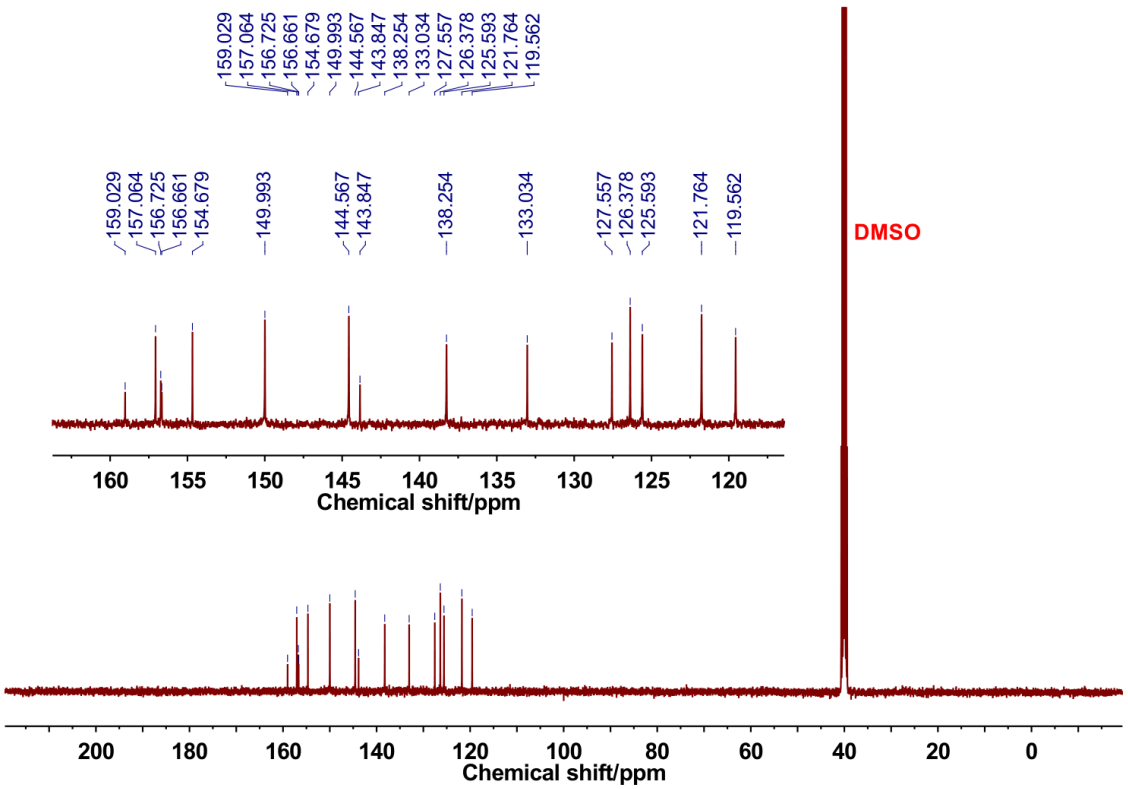

Figure S2. ^{13}C NMR (101 MHz) spectrum of PTP-dq·Cl in DMSO-d$_6$.

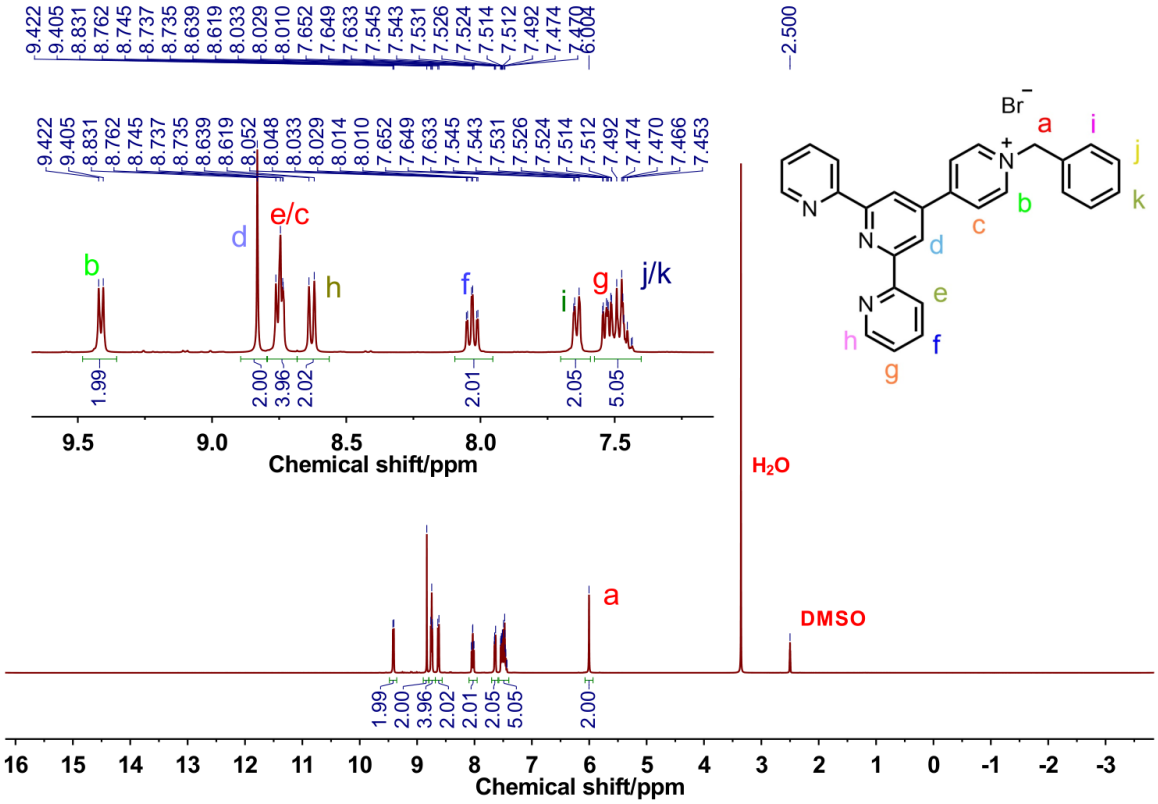

Figure S3. ^{1}H NMR (400 MHz) spectrum of PTP-xb·Br in DMSO-d$_6$.

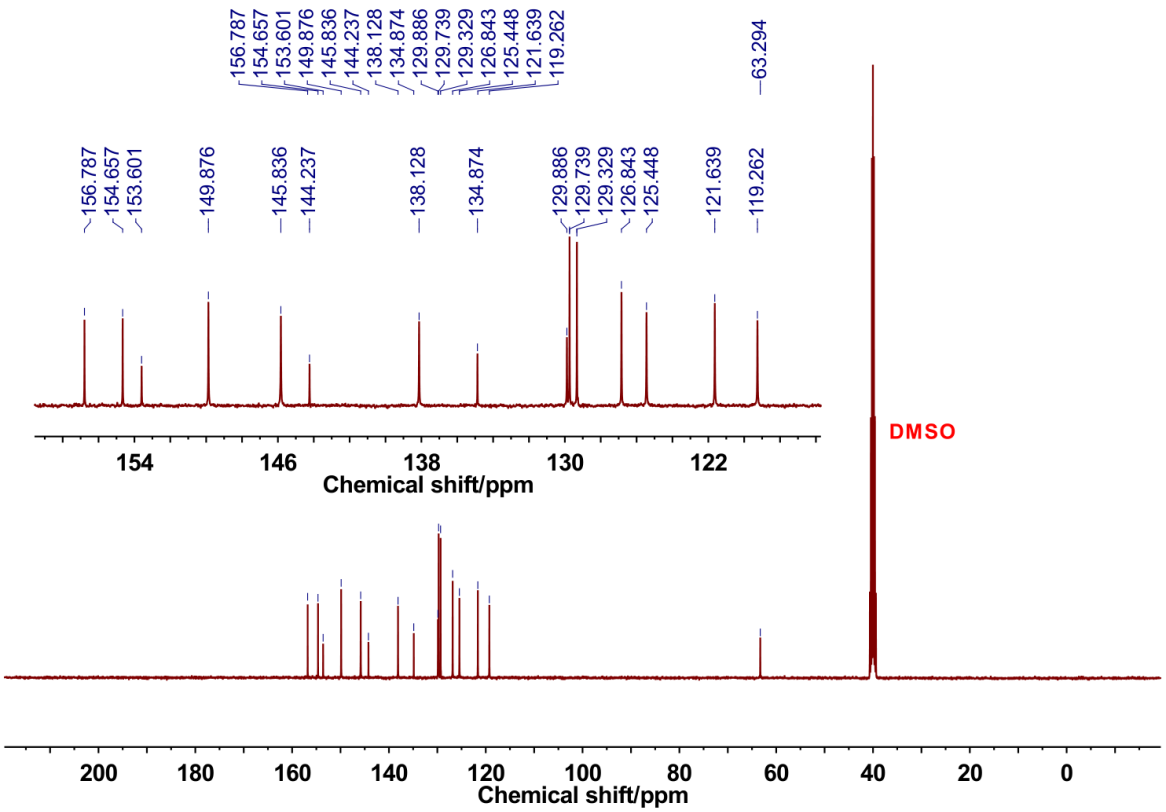

Figure S4. ^{13}C NMR (101 MHz) spectrum of PTP-xb·Br in DMSO-d_6.

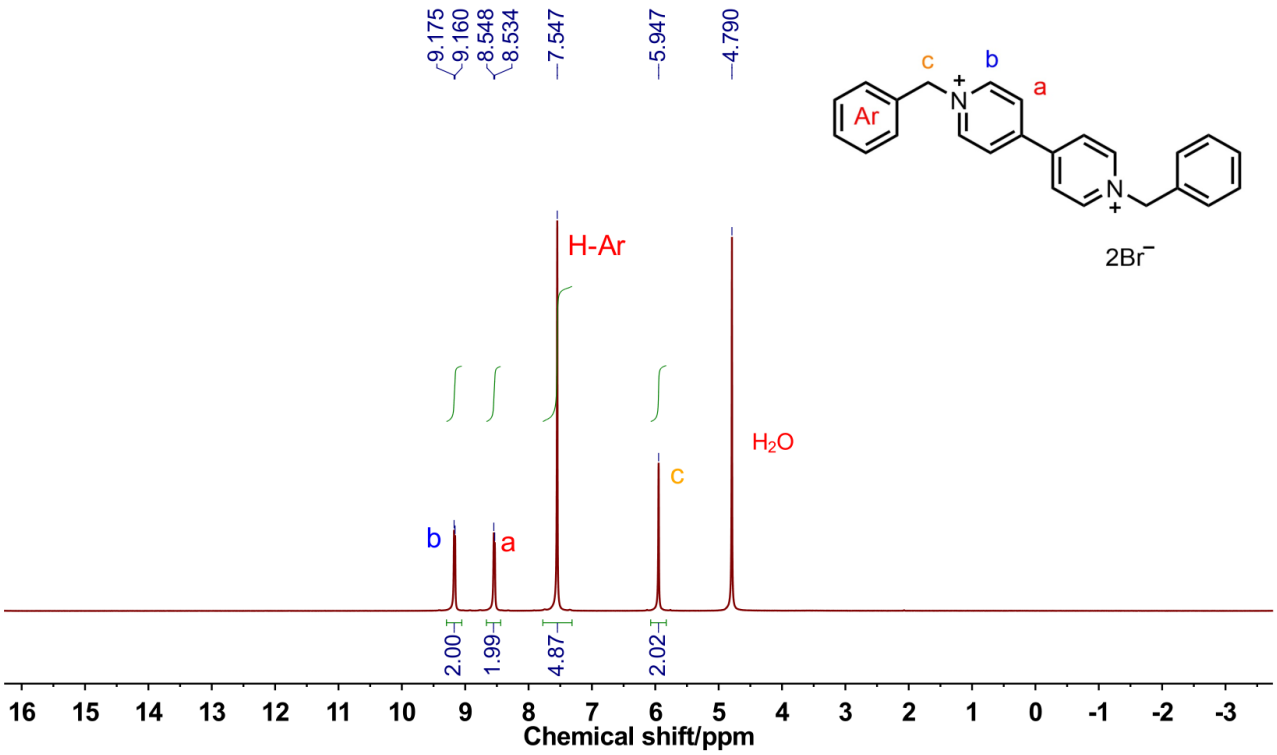

Figure S5. ^{1}H NMR (400 MHz) spectrum of 44bd-2xb·2Br in D_2O.

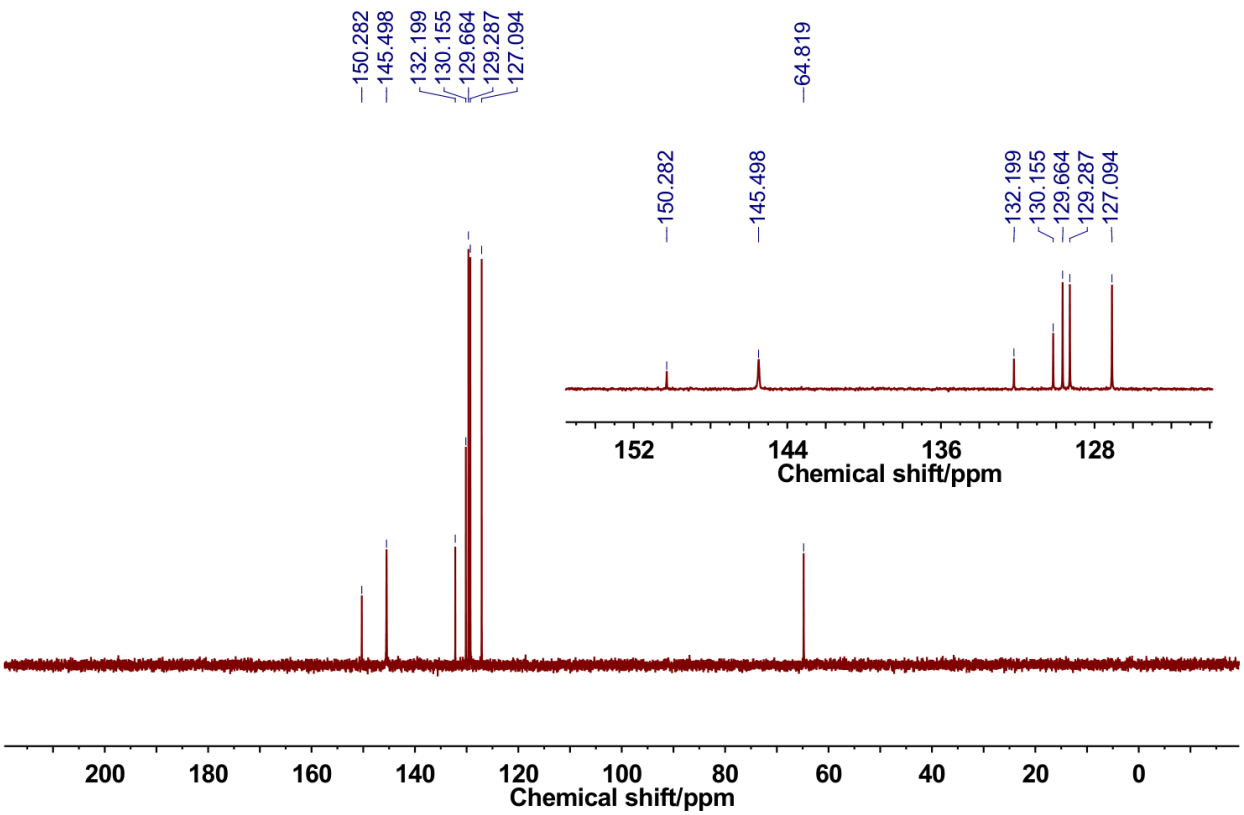

Figure S6. ^{13}C NMR (101 MHz) spectrum of 44bd-2xb·2Br in D_2O.

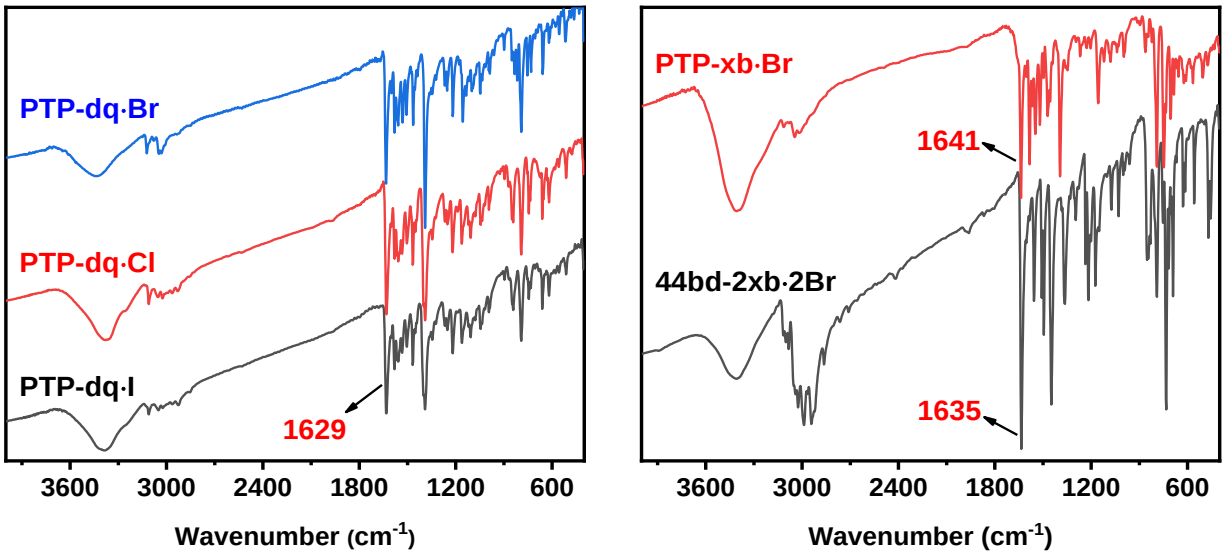

Figure S7. IR spectra of PTP-dq·Cl, PTP-dq·Br, PTP-dq·I, PTP-xb·Br, and 44bd-2xb·2Br.

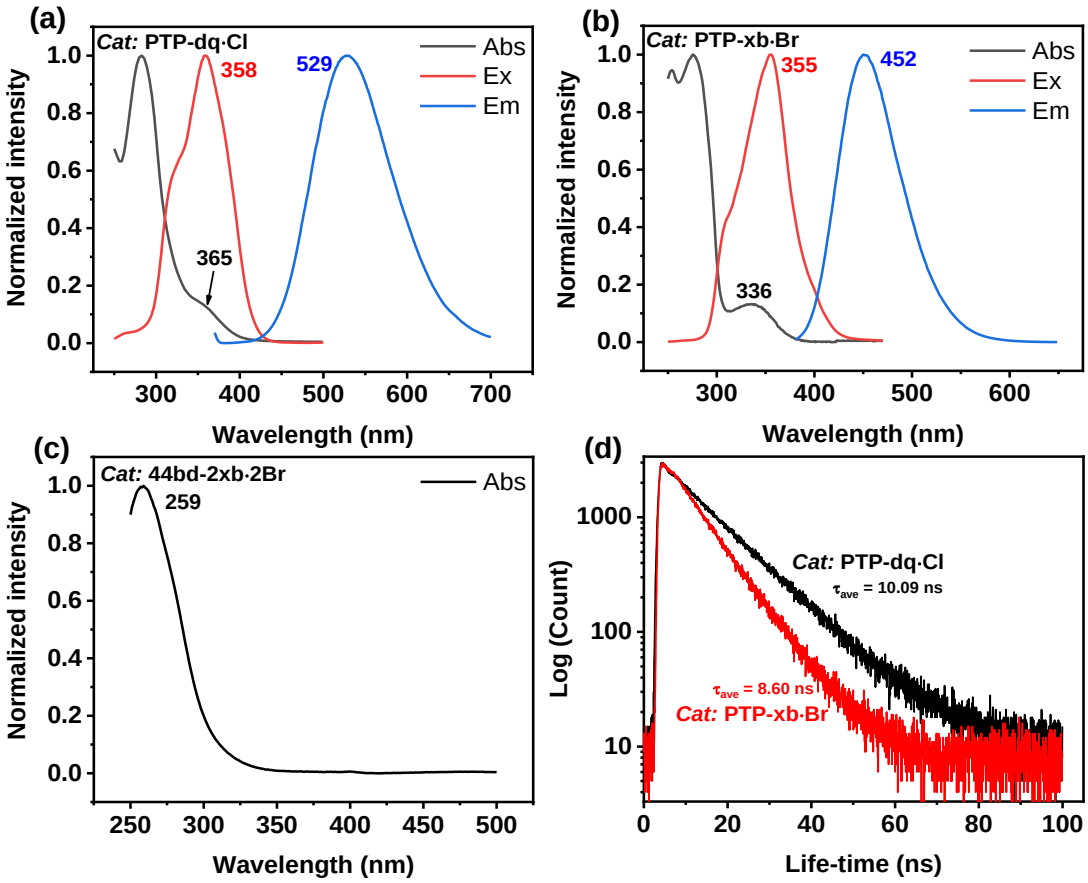

Figure S8. (a-c) Normalized absorption, excitation, and emission spectra of PTP-dq·Cl, PTP-xb·Br, and 44bd-2xb·Br. (d) Fluorescence decays of PTP-dq·Cl and PTP-xb·Br in acetonitrile. Laser excitation wavelength: 320 nm. Abs: absorbance, Ex: excitation, Em: emission. Note: The emission intensity of 44bd-2xb·2Br is too weak to be measured. [1]

[1] R. Ballardini, A. Credi, M. T. Gandolfi, C. Giansante, G. Marconi, S. Silvi, M. Venturi, *Inorganica Chimica Acta* **2007**, *360*, 1072-1082.

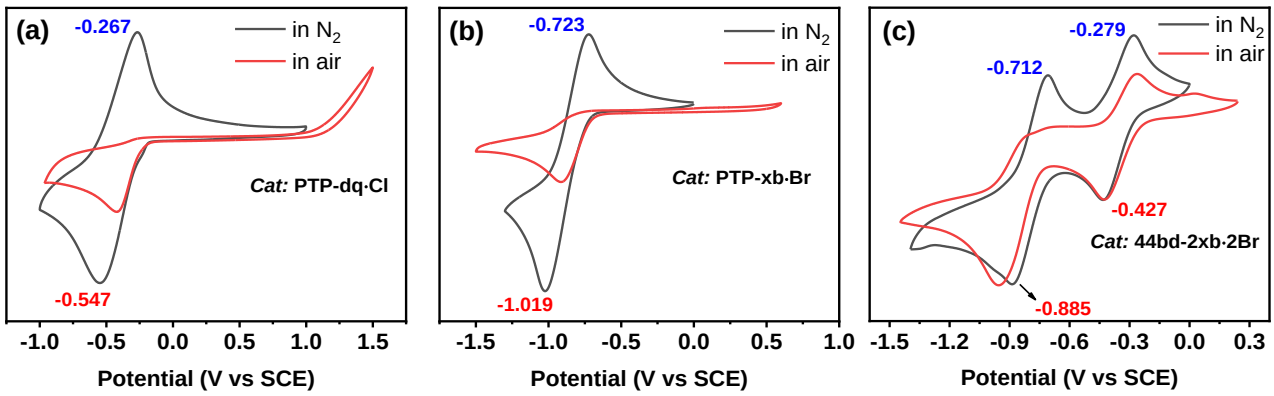

Figure S9. Cyclic voltammograms for photocatalysts PTP-dq·Cl (a), PTP-xb·Br (b) and 44bd-2xb·2Br (c) with the scan rate of 50 mV/s in acetonitrile solution under a N_2 or air atmosphere. The electrolyte is tetrabutylammonium hexafluorophosphate (1.9 mmol/L).

Section 4. Additional figures

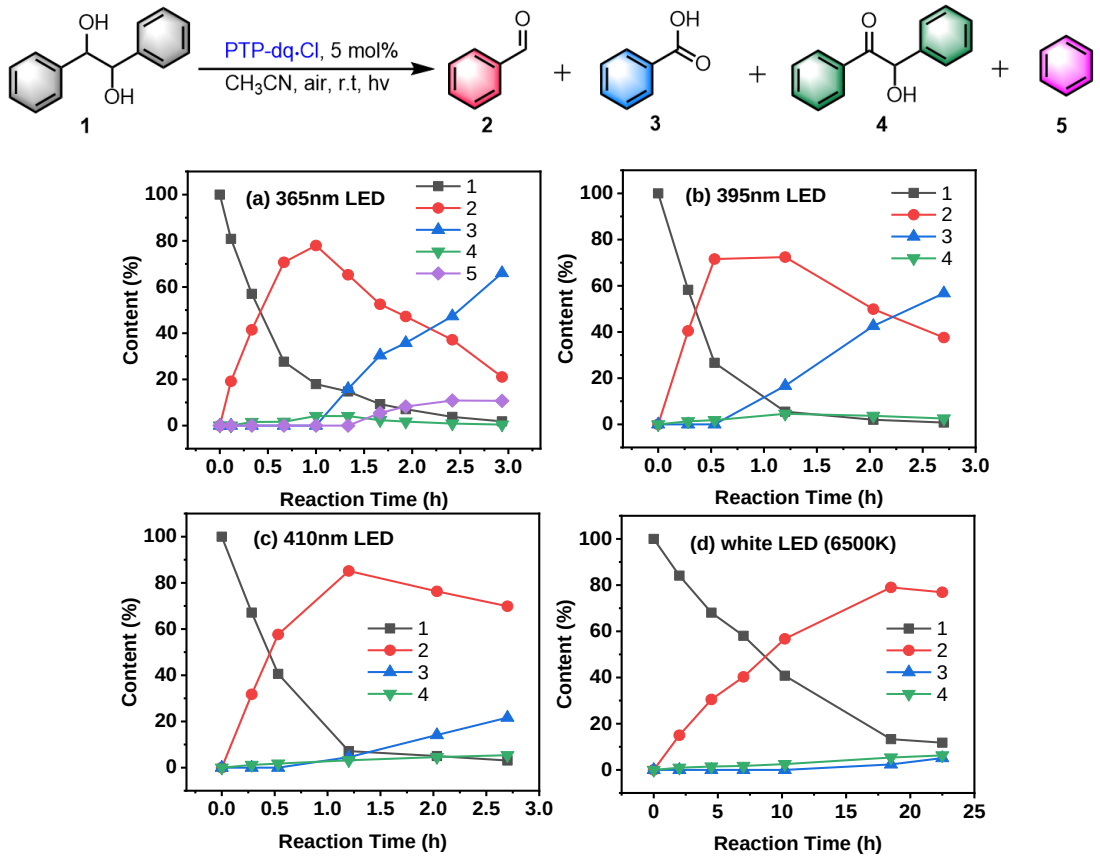

Figure S10. Time-dependent conversion of 1,2-diphenylethane-1,2-diol (**1**) under different light sources. Reaction condition: substrate (0.2 mmol) and catalyst **PTP-dq·Cl** (5 mol%) in 5 mL acetonitrile at room temperature under an air atmosphere. The content of products was calculated by the distribution percentage.

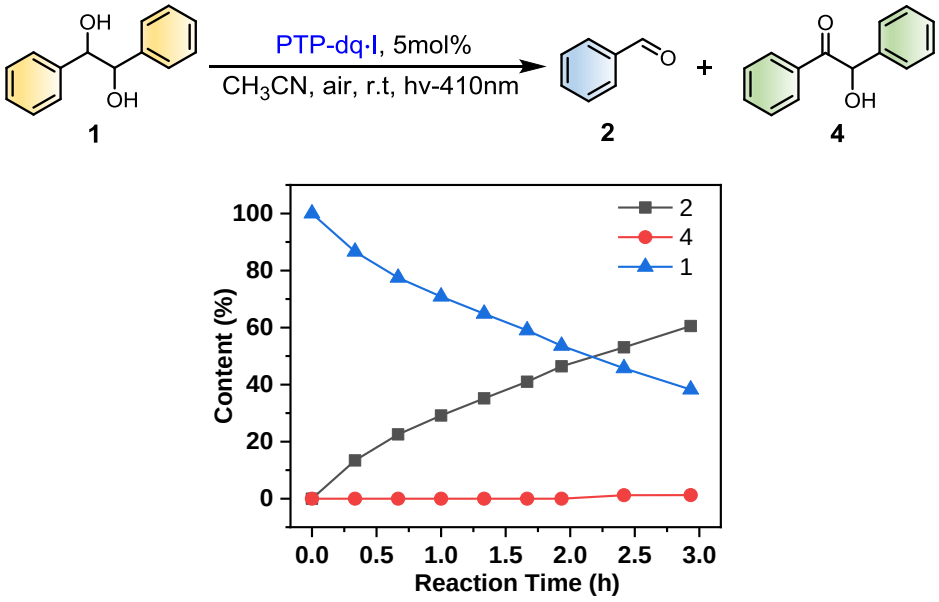

Figure S11. Influence of anions on the conversion of 1,2-diphenylethane-1,2-diol. Reaction condition: substrate (0.2 mmol) and 5 mol% of **PTP-dq·I** in 5 mL acetonitrile at room temperature under an air atmosphere by irradiation with 410 nm light source. The content of products was calculated by the distribution percentage.

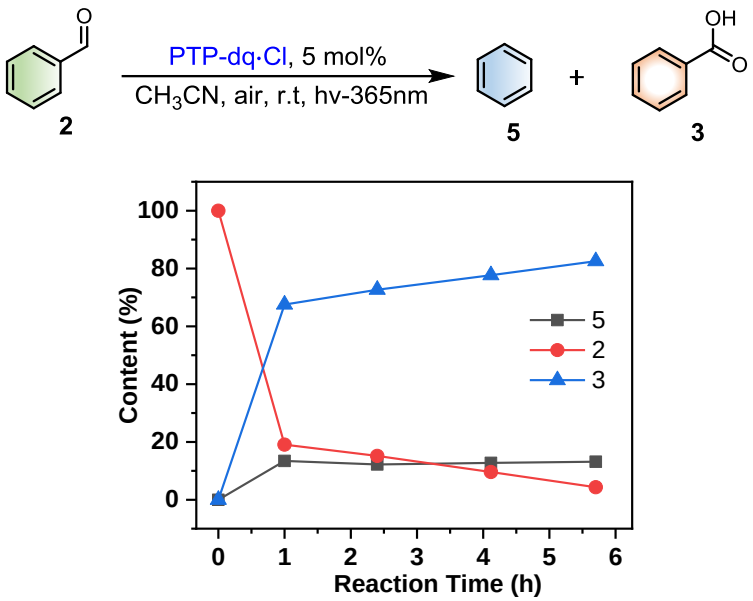

Figure S12. Time-dependent conversion of benzaldehyde. Reaction condition: 0.2 mmol of **2** and 5 mol% of PTP-dq·Cl in 5 mL of acetonitrile at room temperature under an air atmosphere by irradiation with 365 nm light source. The content of products was calculated by the distribution percentage.

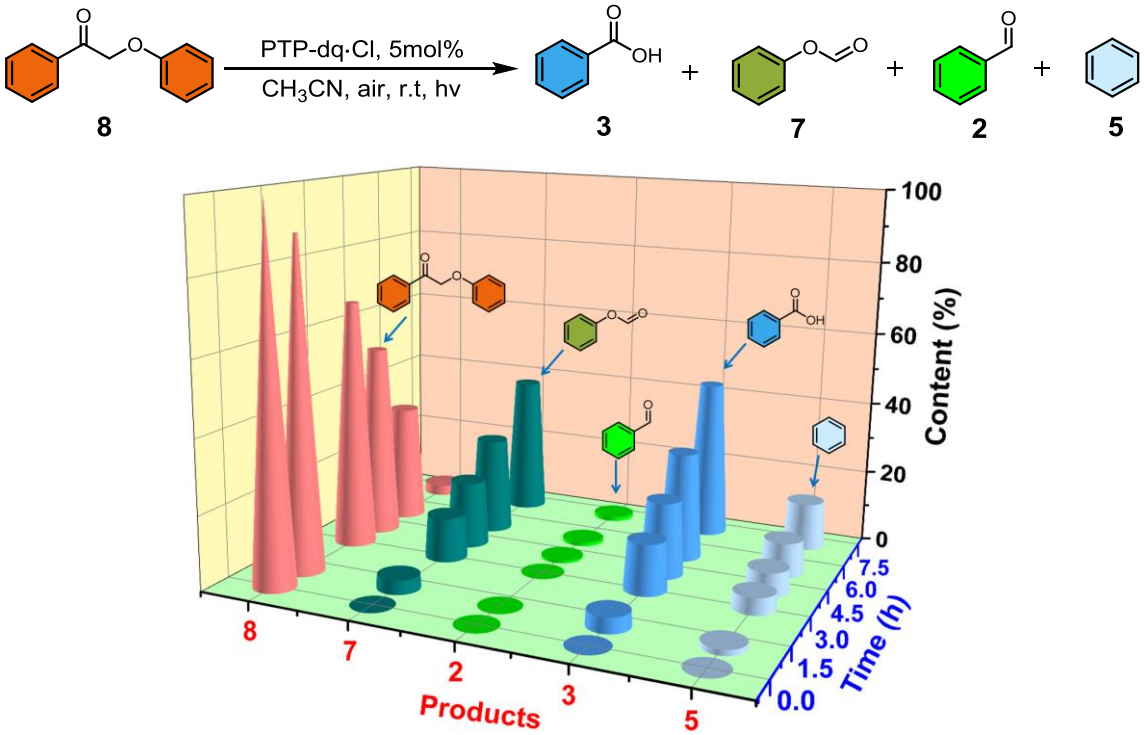

Figure S13. Time-dependent conversion of 2-phenoxy-1-phenylethanone (**8**). Reaction condition: **8** (0.2 mmol), catalyst PTP-dq·Cl (5 mol%) in 5 mL acetonitrile at room temperature under an air atmosphere by irradiation with 365 nm light source. The content of products was calculated by the distribution percentage.

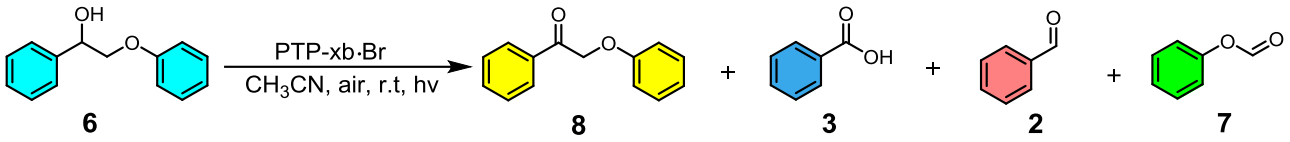

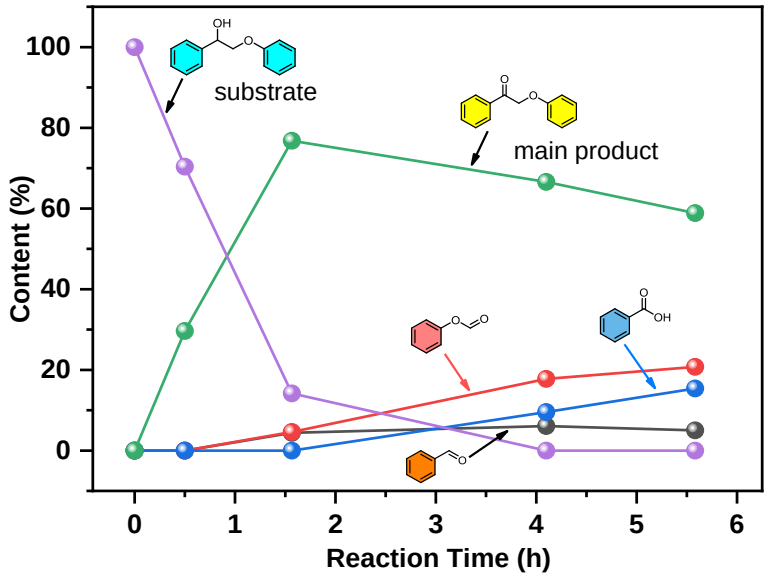

Figure S14. Time-dependent conversion of 2-phenoxy-1-phenylethanol (**6**). Reaction condition: **6** (0.2 mmol), catalyst PTP-xb·Br (5 mol%) in 5 mL acetonitrile at room temperature under an air atmosphere by irradiation with 365 nm light source. The content of products was calculated by the distribution percentage.

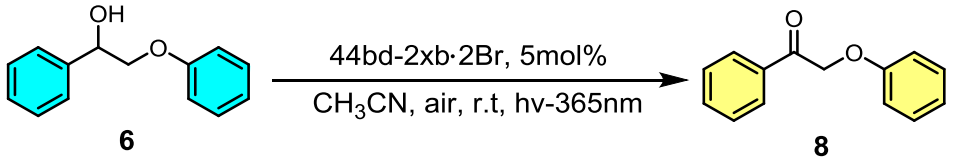

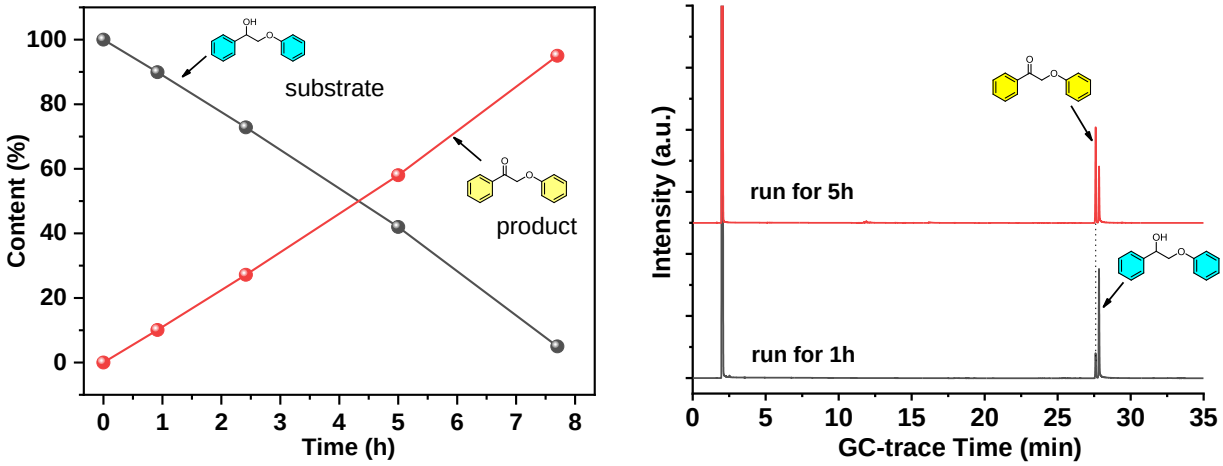

Figure S15. (left) Photocatalytic conversion of 2-phenoxy-1-phenylethanol. Reaction condition: substrate (0.2 mmol), catalyst 44bd-2xb·2Br (5 mol%) in 5 mL acetonitrile at room temperature under an air atmosphere, by irradiation with 365 nm light source. The content of products was calculated by the distribution percentage. (right) GC trace time of this reaction at different reaction time.

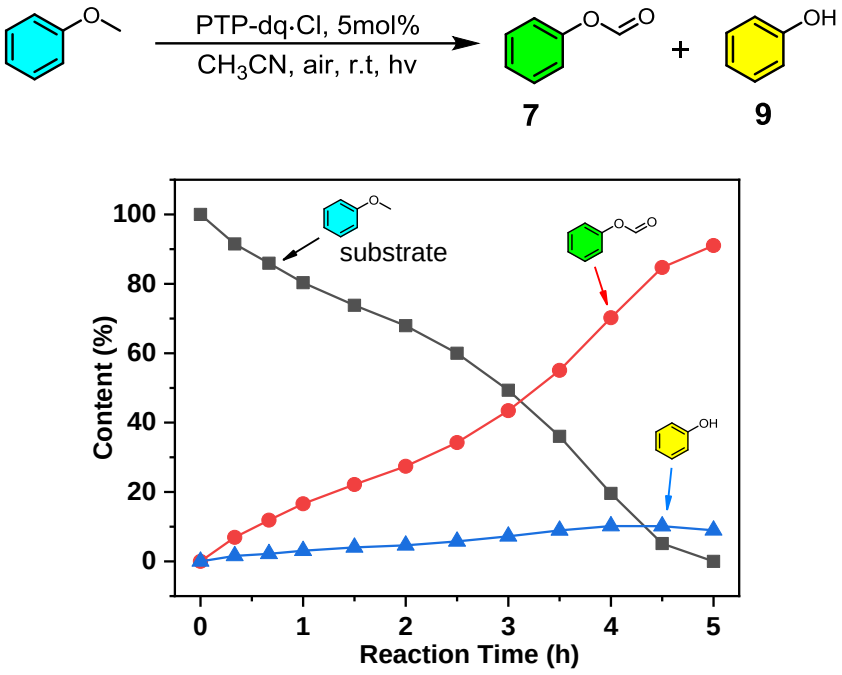

Figure S16. Time-dependent conversion of anisole. Reaction condition: anisole (0.2 mmol), catalyst PTP-dq·Cl (5 mol%) in 5 mL acetonitrile at room temperature under an air atmosphere by irradiation with 365 nm light source. The content of products was calculated by the distribution percentage.

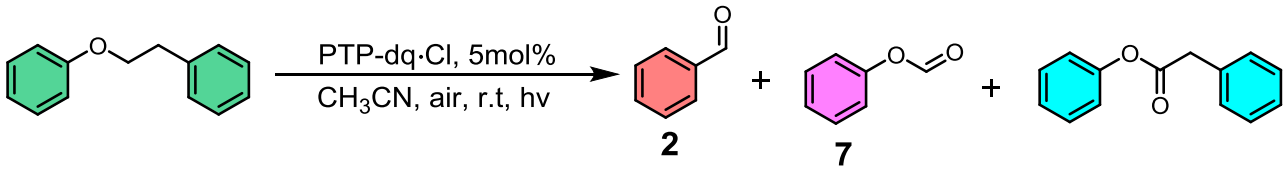

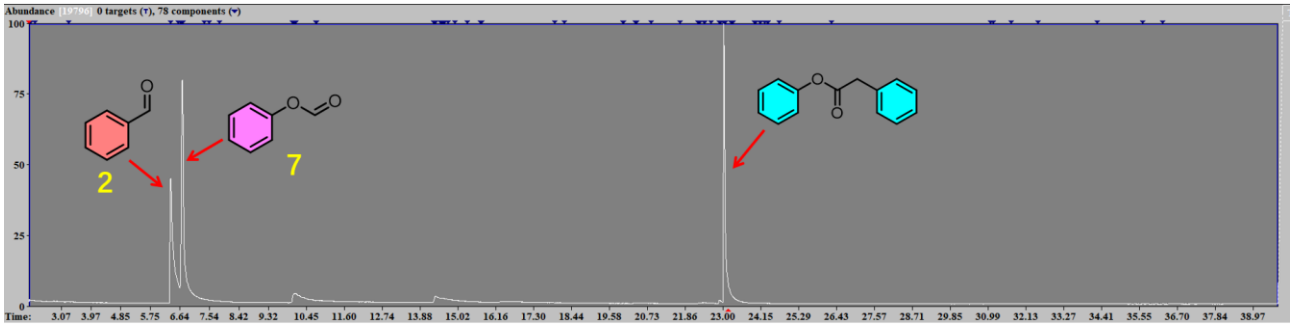

Figure S17. GC-Mass trace of crude reaction mixture of the photochemical reaction of 2-phenylethyl phenyl ether. Reaction conditions: 0.2 mmol of substrate and 5 mol% of PTP-dq·Cl in 5 mL of acetonitrile at room temperature under an air atmosphere, by irradiation with 365 nm light source for 5h.

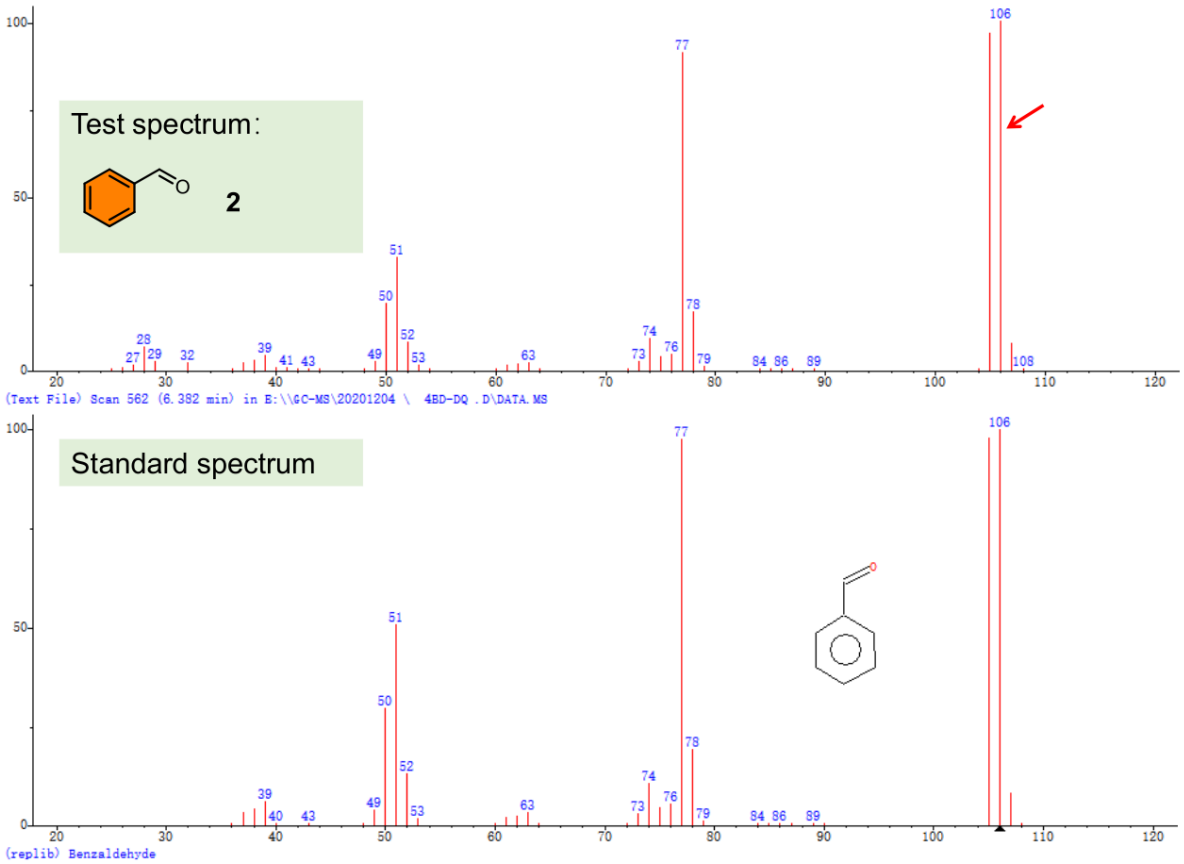

Figure S18. GC-Trace time at 6.382min; MS: 106 for the product benzaldehyde (**2**).

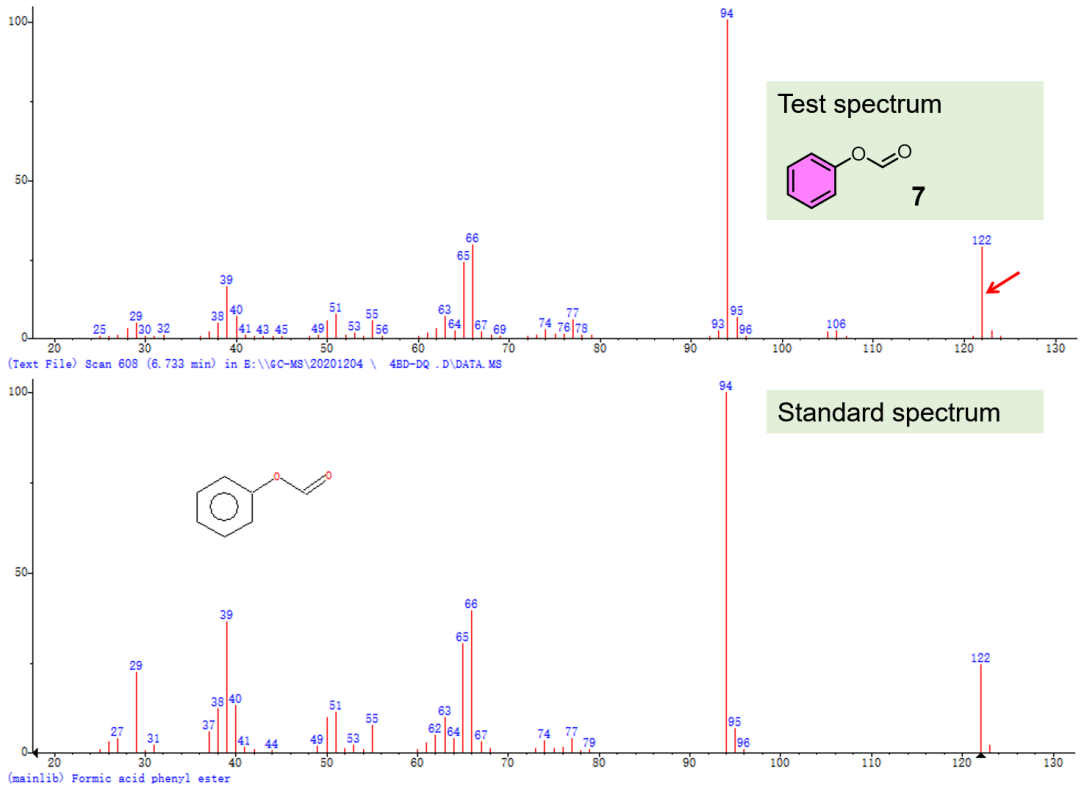

Figure S19. GC-Trace time at 6.733min; MS: 122 for the product phenyl formate (**9**).

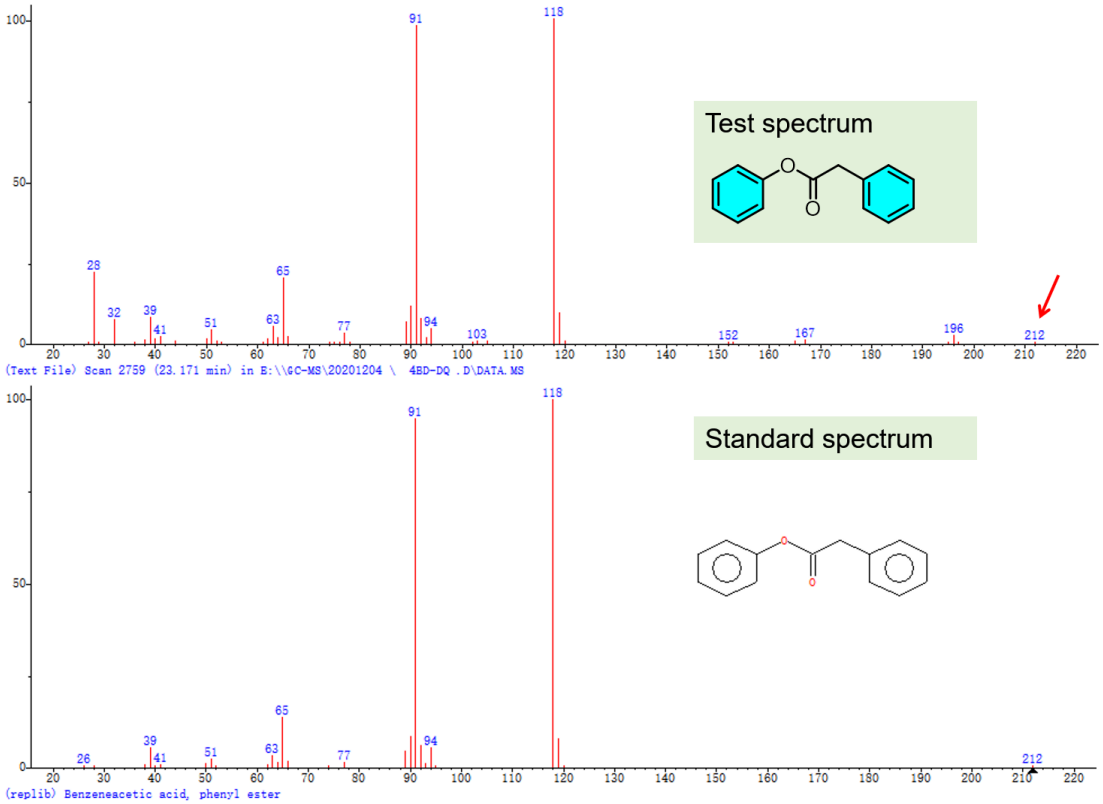

Figure S20. GC-Trace time at 23.171min; MS: 212 for the product phenyl 2-phenylacetate.

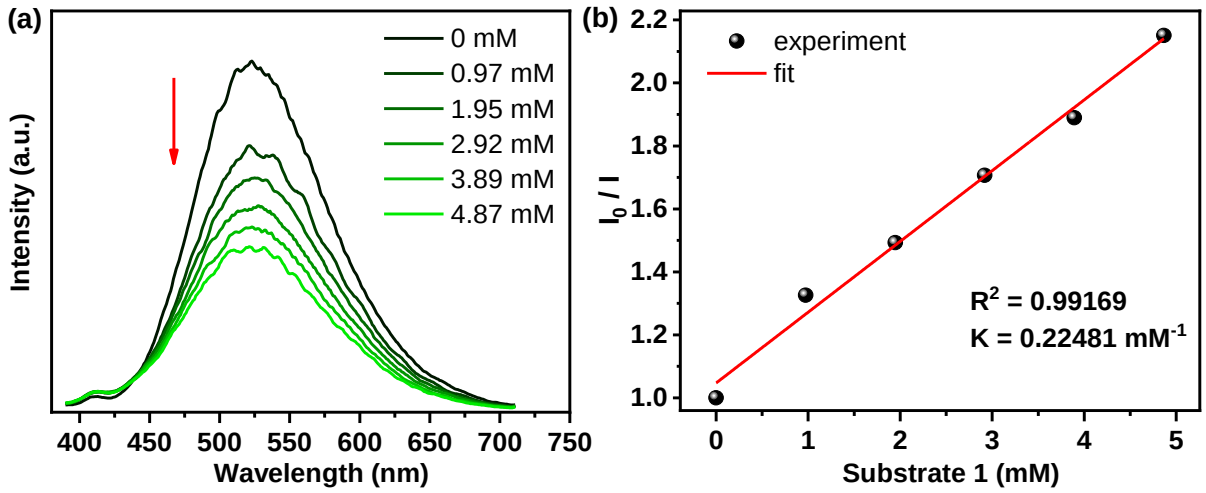

Figure S21. (a) Fluorescence emission spectral change of PTP-dq·Cl (50 μM) in the presence of increasing amount of 1,2-diphenylethane-1,2-diol (**1**) (0~4.87mM) in CH_3CN (λex = 365 nm). (b) Stern-Volmer quenching plot for relative fluorescence intensity of PTP-dq·Cl with increasing concentration of **1**.

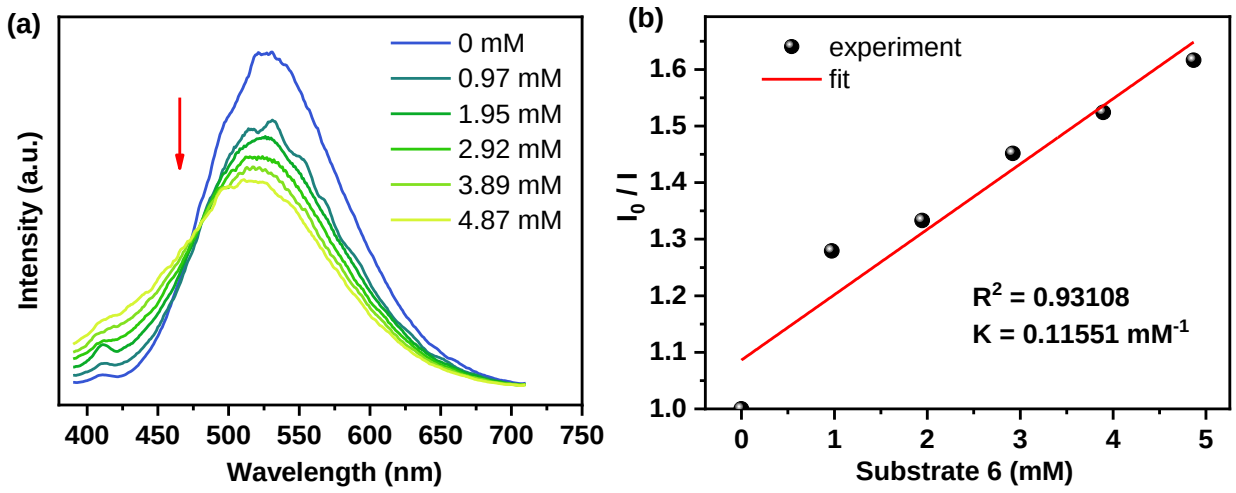

Figure S22. (a) Fluorescence emission spectral change of PTP-dq·Cl (50 μM) in the presence of increasing amount of 2-phenoxy-1-phenylethanol (**6**) (0~4.87mM) in CH_3CN (λex = 365 nm). (b) Stern-Volmer quenching plot for relative fluorescence intensity of PTP-dq·Cl with increasing concentration of **6**.

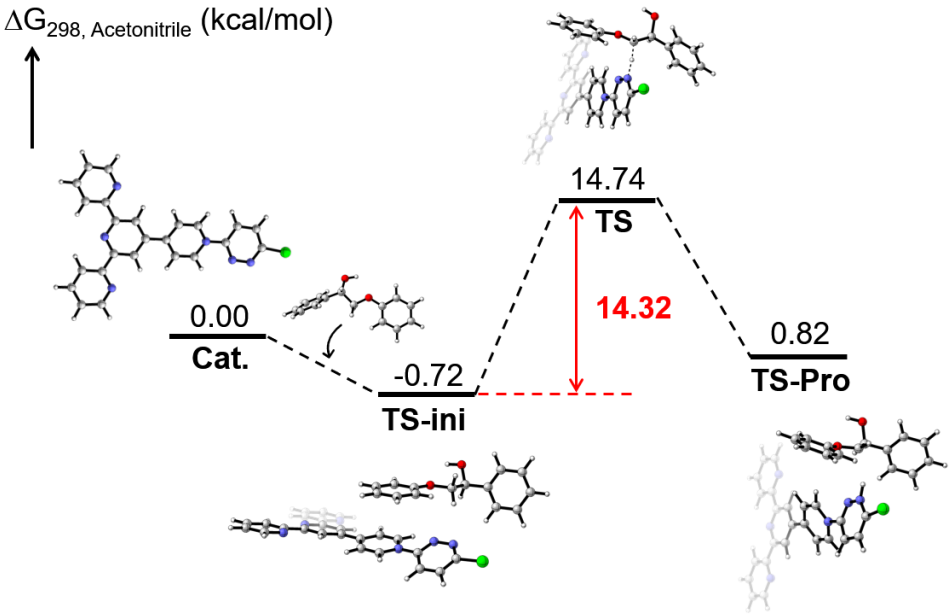

Figure S23. The Gibbs free energy profile (kcal/mol) for the reaction between the C_β–H group of **6** and the N-pyridazine unit (N1) in the singlet state of catalyst (^{1}PTP-dq$^+$*) in CH_3CN. TS-ini, TS and TS-Pro refer to the pre-complex, transition state and post-complex, respectively.

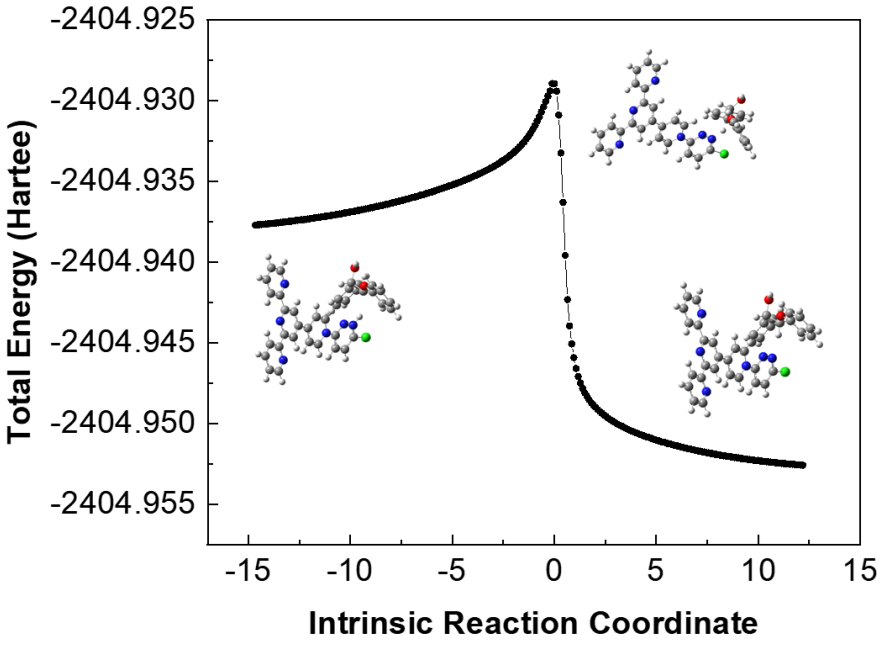

Figure S24. Intrinsic reaction coordinate (IRC) for the PCET transition state in the reaction between the C_β–H group of **6** and the N-pyridazine unit (N1) in the singlet state of catalyst (^{1}PTP-dq$^+$*).

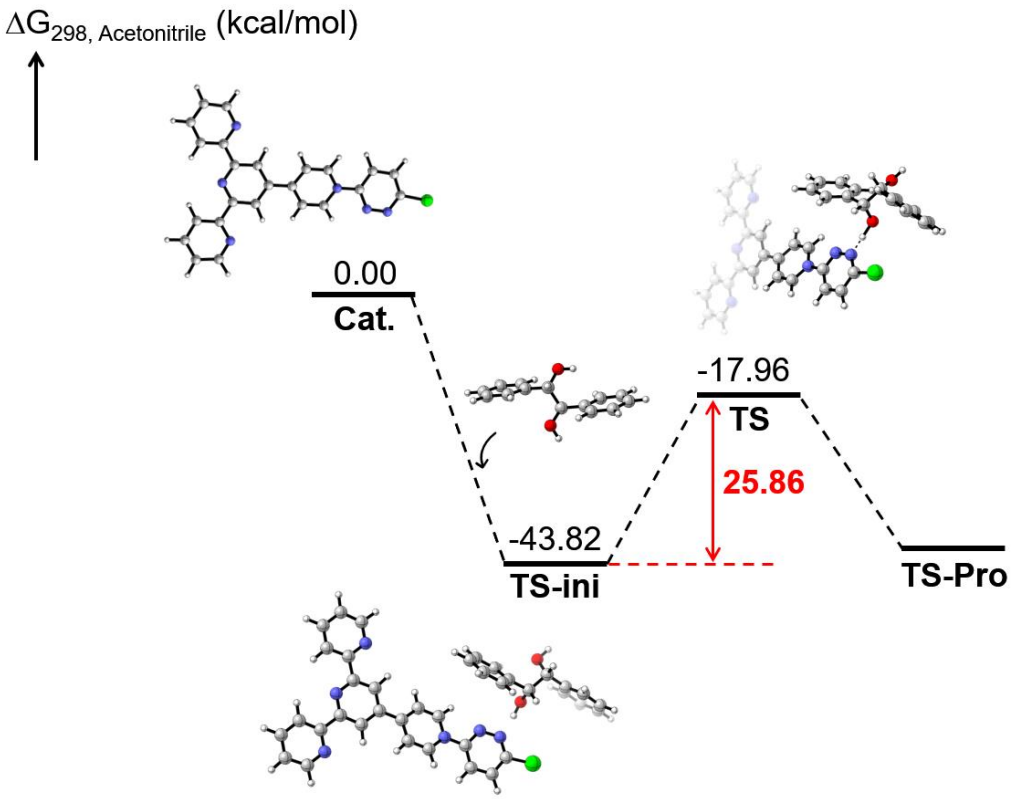

Figure S25. The Gibbs free energy profile (kcal/mol) for the reaction between the C_α–OH group of **1** and the N-pyridazine unit (N1) in the singlet state of catalyst (^{1}PTP-dq$^+$*) in CH_3CN. TS-ini, TS and TS-Pro refer to the pre-complex, transition state and post-complex, respectively.

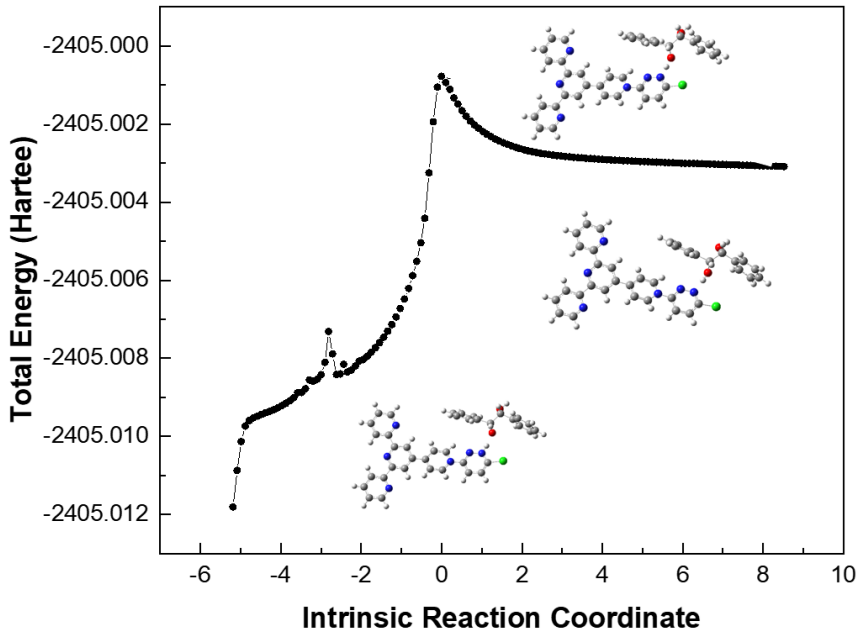

Figure S26. Intrinsic reaction coordinate (IRC) for the PCET transition state in the reaction between the C_{α}–OH group of **1** and the N-pyridazine unit (N1) in the singlet state of catalyst (^{1}PTP-dq^{+}*).

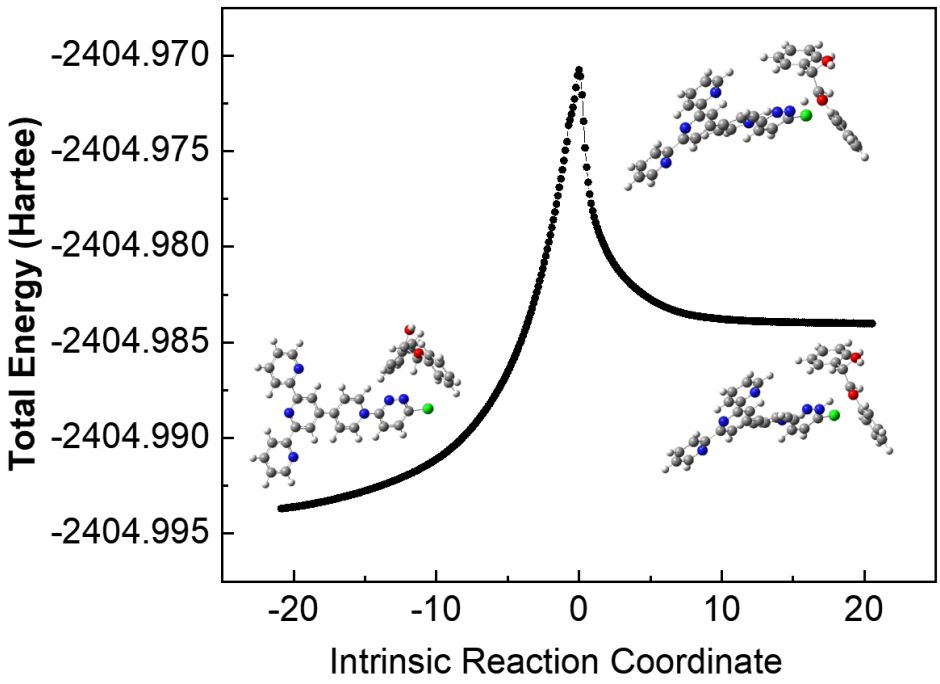

Figure S27. Intrinsic reaction coordinate (IRC) for the PCET transition state in the reaction between the C_{β}–H group of **6** and the N-pyridazine unit (N1) in the triplet state of catalyst (^{3}PTP-dq^{+}*).

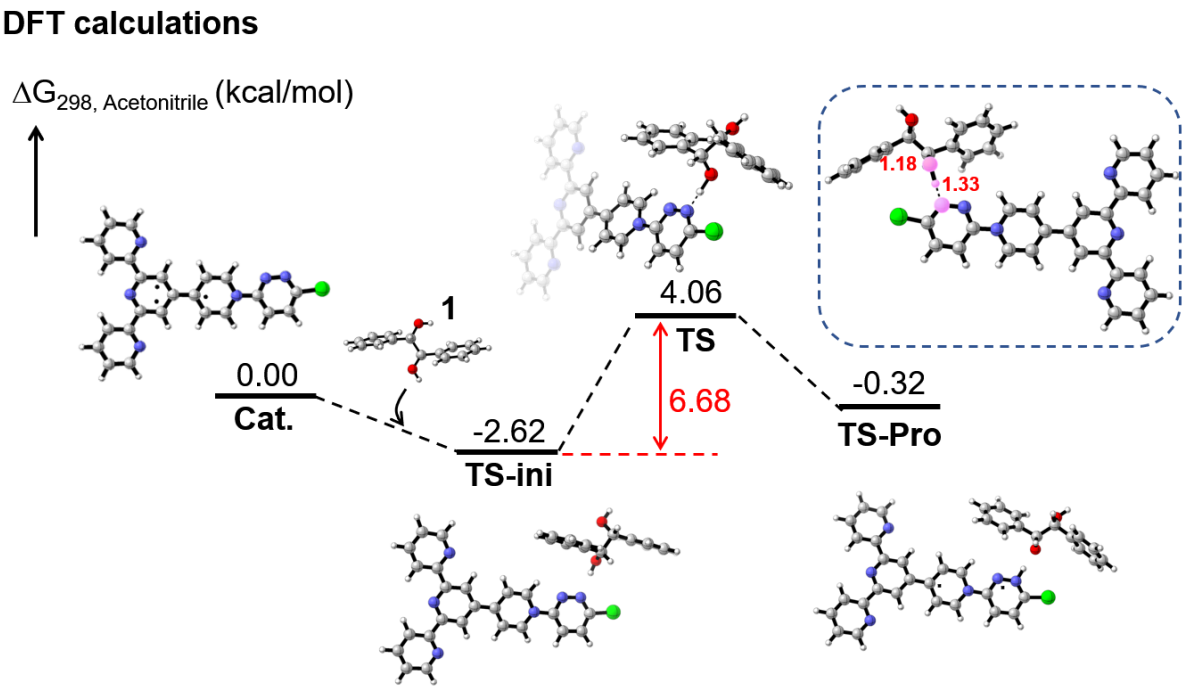

Figure S28. The Gibbs free energy profile (kcal/mol) for the reaction between the C_α–OH group of **1** and the N-pyridazine unit (N1) in the triplet state of catalyst (^{3}PTP-dq$^+$*) in CH_3CN. TS-ini, TS and TS-Pro refer to the pre-complex, transition state and post-complex, respectively.

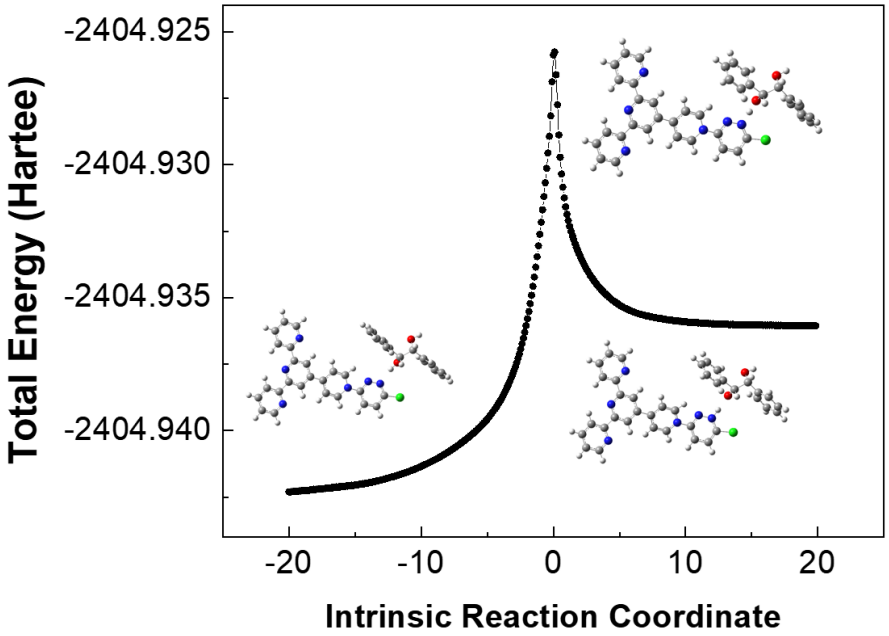

Figure S29. Intrinsic reaction coordinate (IRC) for the PCET transition state in the reaction between the C_α–OH group of **1** and the N-pyridazine unit (N1) in the triplet state of catalyst (^{3}PTP-dq$^+$*).

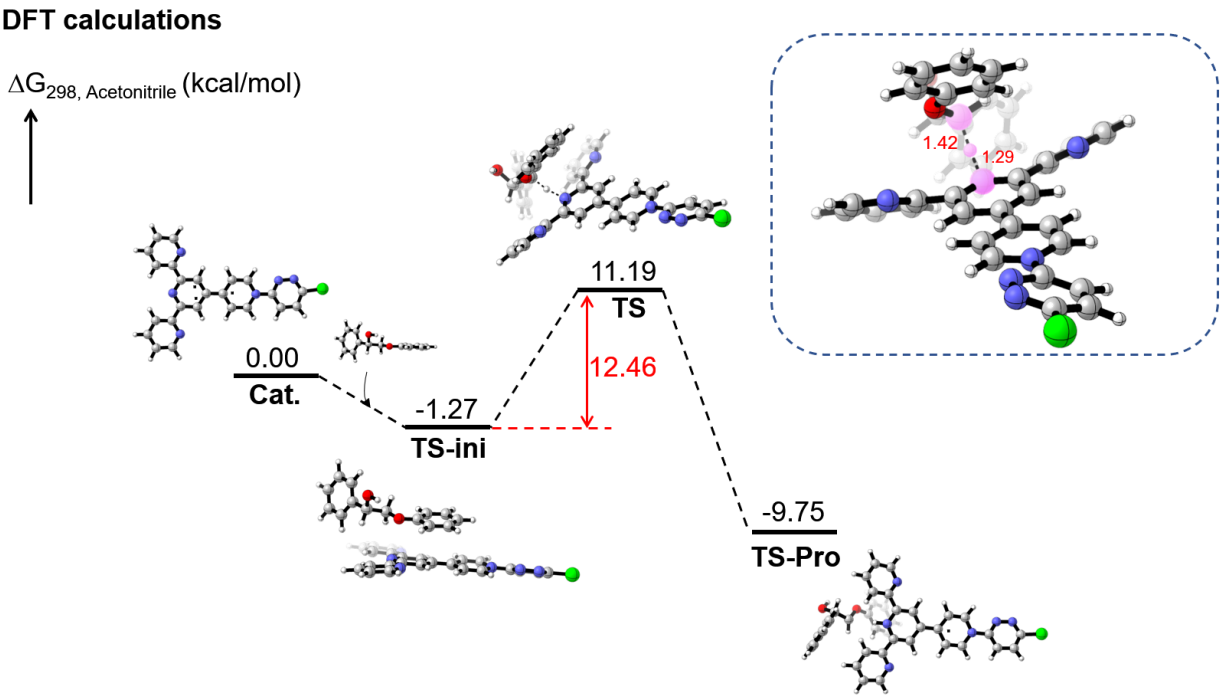

Figure S30. The Gibbs free energy profile (kcal/mol) for the reaction between the C_β–H group of **6** and the N-pyridine unit (N2) in the triplet state of catalyst (^{3}PTP-dq$^+$*) in CH_3CN. TS-ini, TS and TS-Pro refer to the pre-complex, transition state and post-complex, respectively.

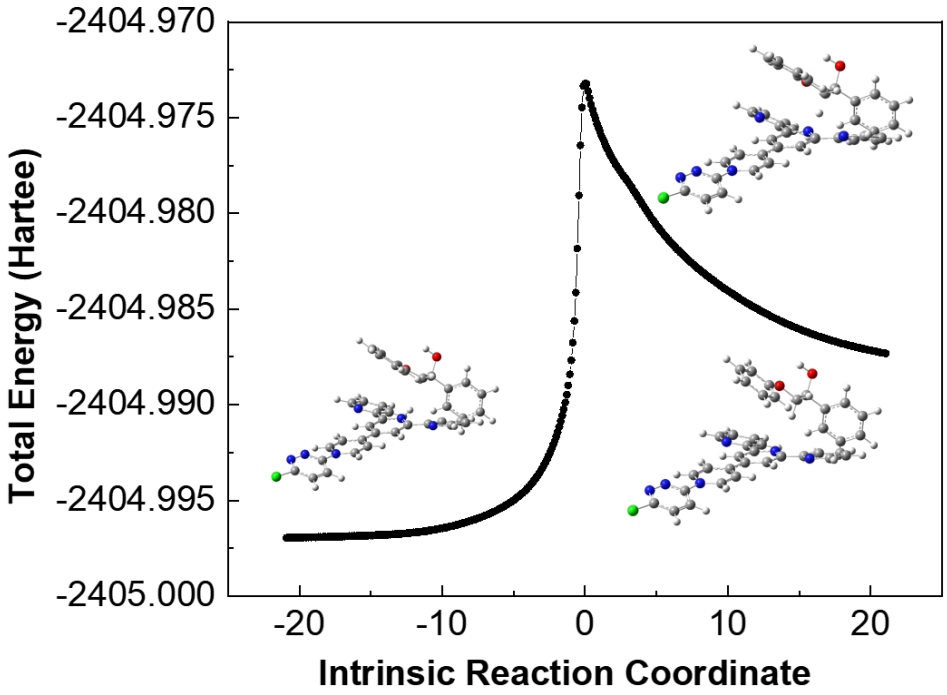

Figure S31. Intrinsic reaction coordinate (IRC) for the PCET transition state in the reaction between the C_β–H group of **6** and the N-pyridine unit (N2) in the triplet state of catalyst (^{3}PTP-dq$^+$*).

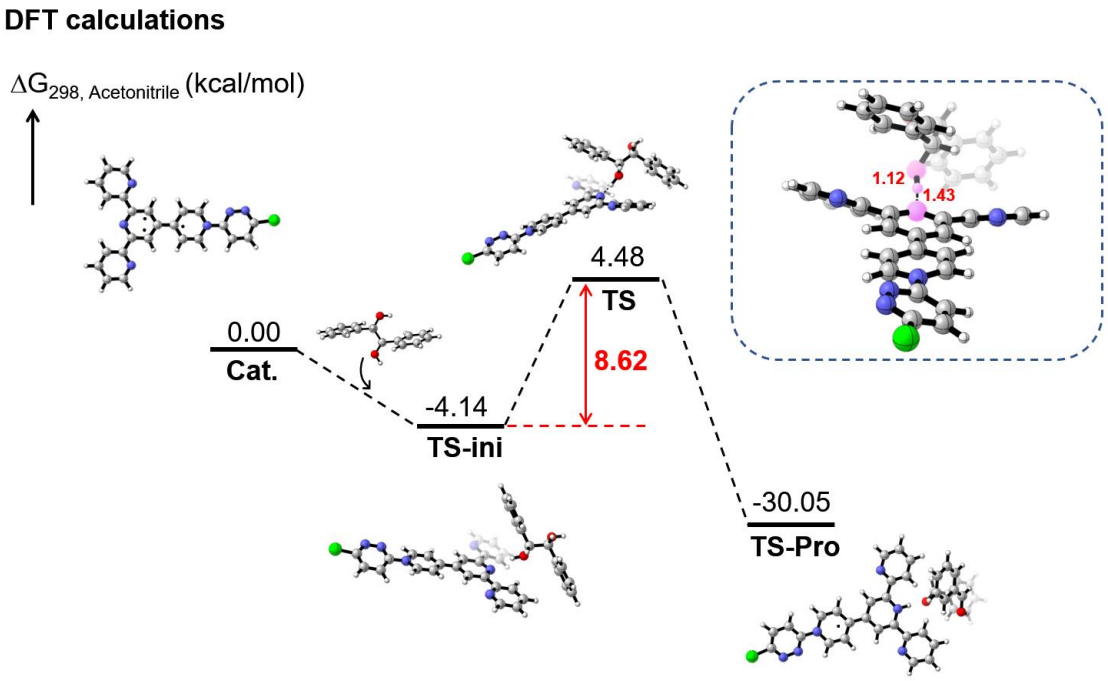

Figure S32. The Gibbs free energy profile (kcal/mol) for the reaction between the C_α–OH group of **1** and the N-pyridine unit (N2) in the triplet state of catalyst (^{3}PTP-dq$^+$*) in CH_3CN. TS-ini, TS and TS-Pro refer to the pre-complex, transition state and post-complex, respectively.

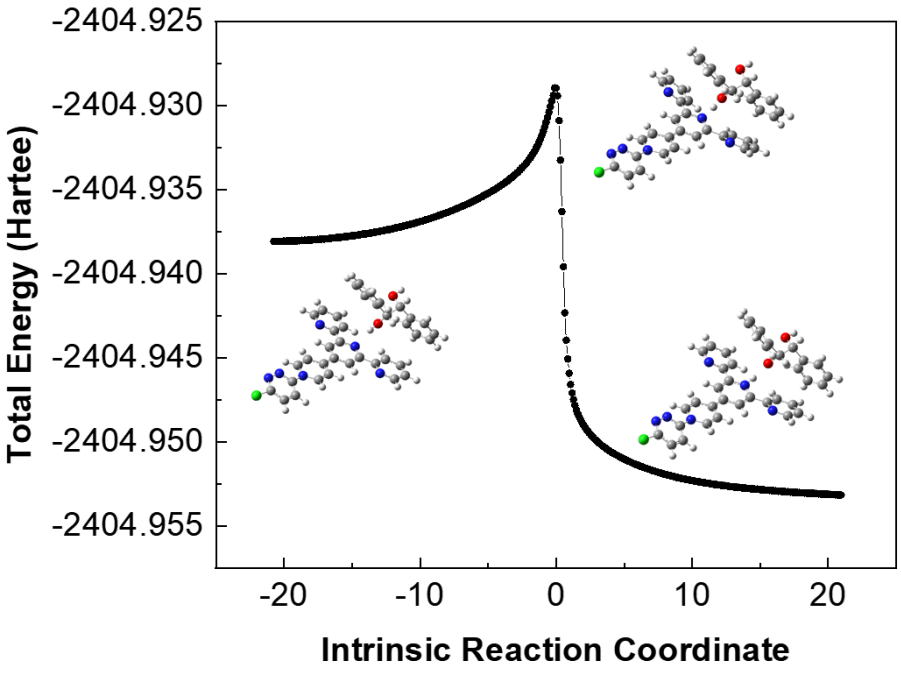

Figure S33. Intrinsic reaction coordinate (IRC) for the PCET transition state in the reaction between the C_α–OH group of **1** and the N-pyridine unit (N2) in the triplet state of catalyst (^{3}PTP-dq$^+$*).

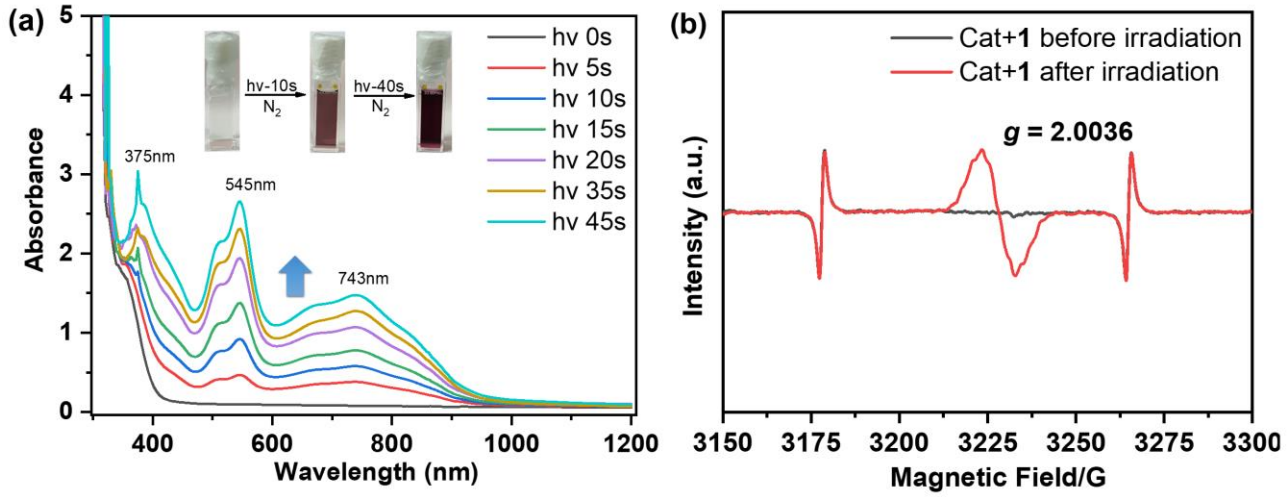

Figure S34. (a) UV-vis absorption spectral change of PTP-dq·Cl in the presence of 1,2-diphenylethane-1,2-diol (**1**) in CH_3CN under a N_2 atmosphere upon 365 nm light irradiation. Inset: showing the color change of reaction mixture under light irradiation. (b) ESR spectral change of the mixture of PTP-dq·Cl and **1** in acetonitrile under a N_2 atmosphere before (black line) and after (red line) 365 nm light irradiation. The signals of the Mn (II) ion as internal standard are shown on the two sides for comparison.

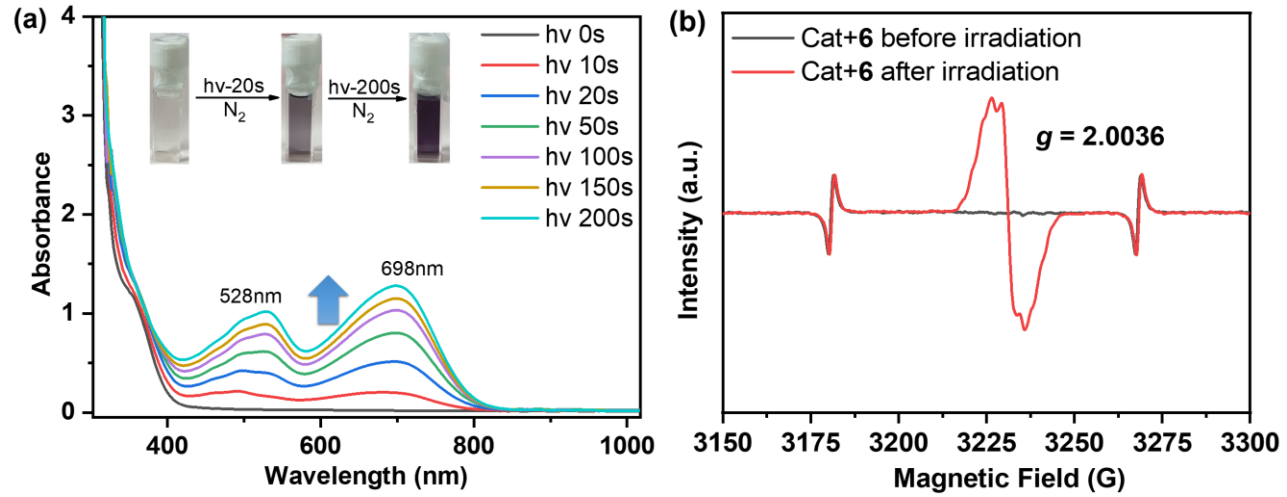

Figure S35. (a) UV-vis absorption spectral change of PTP-dq·Cl in the presence of **6** in CH_3CN under a N_2 atmosphere and irradiated by 365 nm light source. Inset: showing the color change of reaction mixture under light irradiation. (b) ESR spectral change of the mixture of PTP-dq·Cl and **6** in acetonitrile under a N_2 atmosphere before (black line) and after (red line) 365 nm light irradiation. The signals of the Mn (II) ion as internal standard are shown on the two sides for comparison.

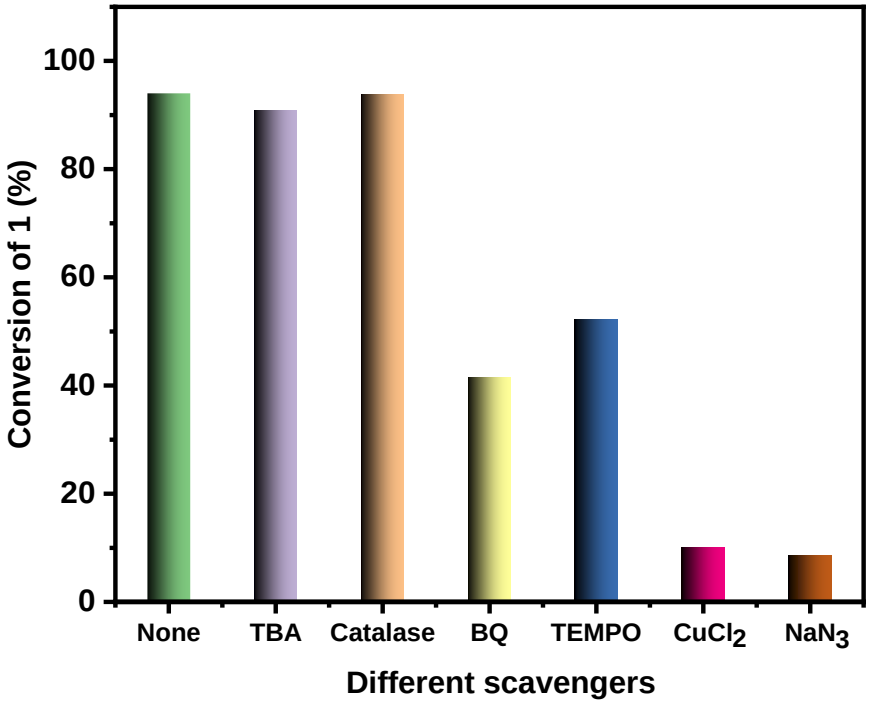

Figure S36. Inhibition impact of different scavengers on the conversion of **1**. Reaction condition: 0.2 mmol of **1**, 5 mol% PTP-dq·Cl and 30 mol% scavengers in 5 mL acetonitrile at room temperature under air atmosphere, irradiation by 410 nm light source for 90 min. *p*-benzoquinone (BQ), tert-butanol (TBA), catalase, and NaN_3 as the scavengers to probe the $^{\bullet}O_2^-$, $^{\bullet}OH$, H_2O_2, and $^1O_2$, respectively.

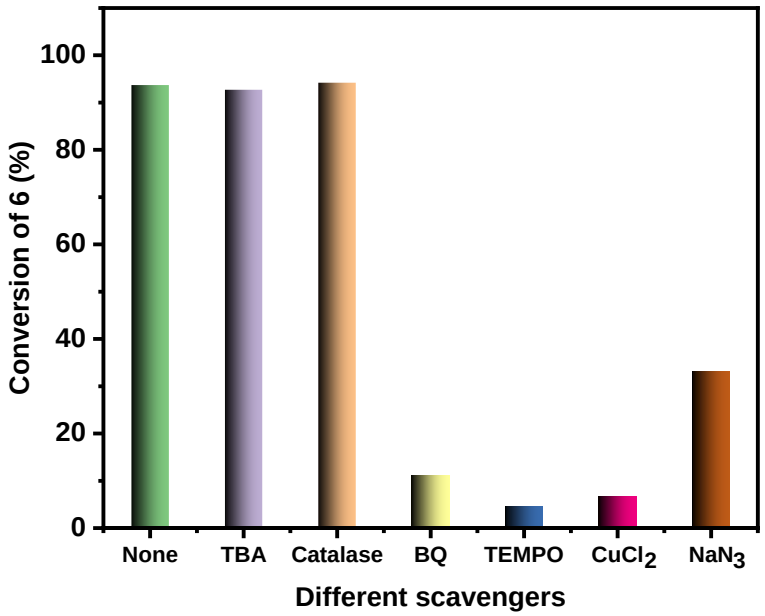

Figure. S37. Inhibition impact of different scavengers on the conversion of **6**. Reaction condition: 0.2 mmol of **6**, 5 mol% of **PTP-dq·Cl** and 30 mol% of scavengers in 5 mL acetonitrile at room temperature under air atmosphere, irradiation by 365 nm light source for 6 h. *p*-benzoquinone (BQ), tert-butanol (TBA), catalase, and NaN_3 as the scavengers to probe the $^{\bullet}O_2^-$, $^{\bullet}OH$, H_2O_2, and $^1O_2$, respectively.

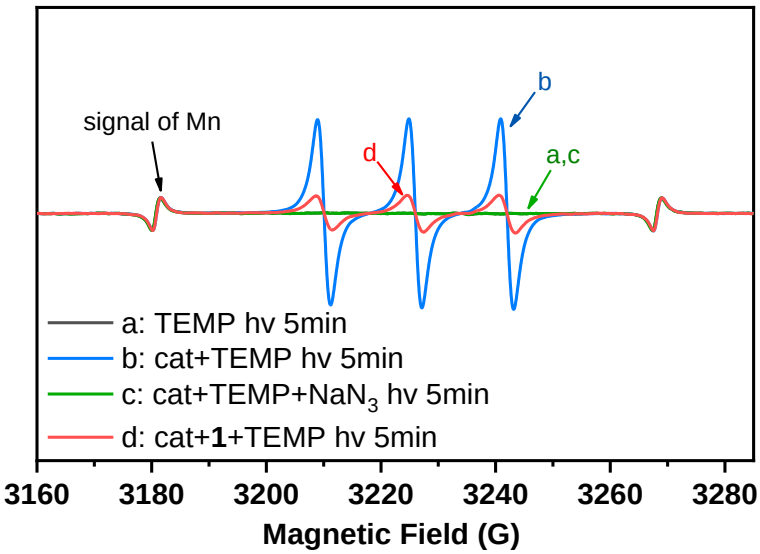

Figure S38. ESR spectra for the mixture of catalyst PTP-dq·Cl (1 mg), substrate **1** (4 μL), NaN_3 (1 mg), and TEMP (1 mg) in 1 mL of acetonitrile, irradiation with 365 nm light source under air at room temperature. The signals of the Mn (II) ion as internal standard are shown on the two sides for comparison. Note: A group of significant triple peak signals of TEMP-$^1O_2$ adduct appeared in the reaction solution when catalyst PTP-dq·Cl and TEMP ($^1O_2$ trapping agent) exist together. Quenching effect of NaN_3 further confirmed the capability of PTP-dq·Cl for $^1O_2$ generation. Additionally, the signal intensity of $^1O_2$ was significantly reduced due to the interaction between PTP-dq·Cl and substrate **1**.

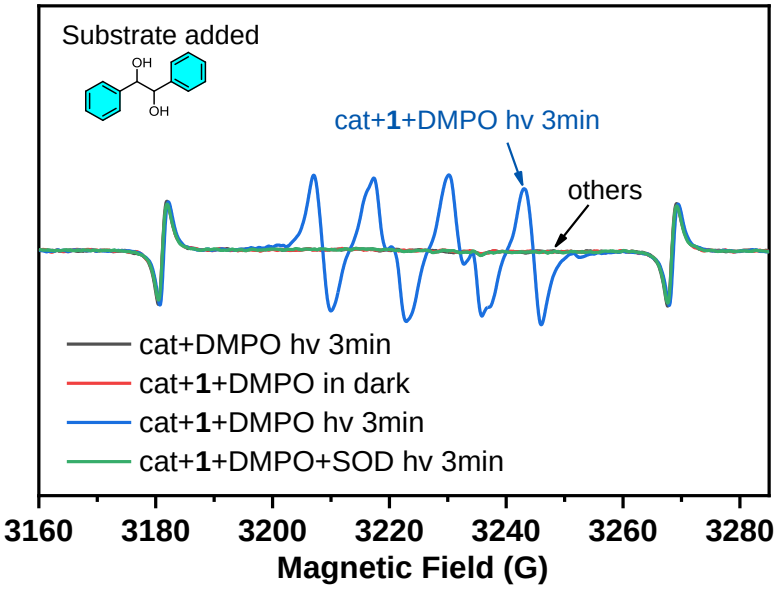

Figure S39. ESR spectra for the mixture of catalyst PTP-dq·Cl (1 mg), substrate **1** (4 μL), DMPO (4 μL), and SOD (4 μL) in 1 mL of acetonitrile, irradiation with 365 nm light source under air at room temperature. The signals of the Mn (II) ion as internal standard are shown on the two sides for comparison. Note: No obvious ESR signal was observed when PTP-dq·Cl and 5,5-dimethyl-1-pyrroline N-oxide (DMPO, a radical trapping agent) mixed in acetonitrile whether there was light irradiation. However, a strong1:2:2:1 characteristic ESR signal of DMPO-$^{\bullet}O_2^-$ spin adducts appeared when donor **1** was added. These results indicated that the $^{\bullet}O_2^-$ generation benefits from the electron transfer between catalyst PTP-dq·Cl and **1**.

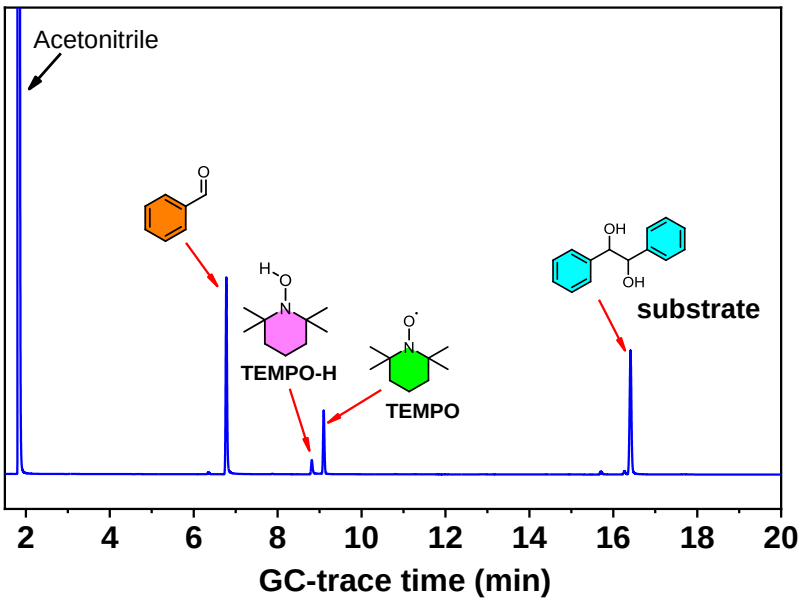

Figure S40. The GC-analysis for the inhibition impact of TEMPO on conversion of **1**. Reaction condition: 0.2 mmol of **1**, 5 mol% of PTP-dq·Cl and 30 mol% of TEMPO in 5 mL of acetonitrile in air at room temperature by irradiation with 410 nm light source for 90 min. GC heating method: The chromatographic column maintains a constant temperature of 100 ℃ for 5 minutes at the beginning. Subsequently, the temperature increases by 15 degrees Celsius per minute to 250 ℃. Lastly, the temperature lasts for 10 min.

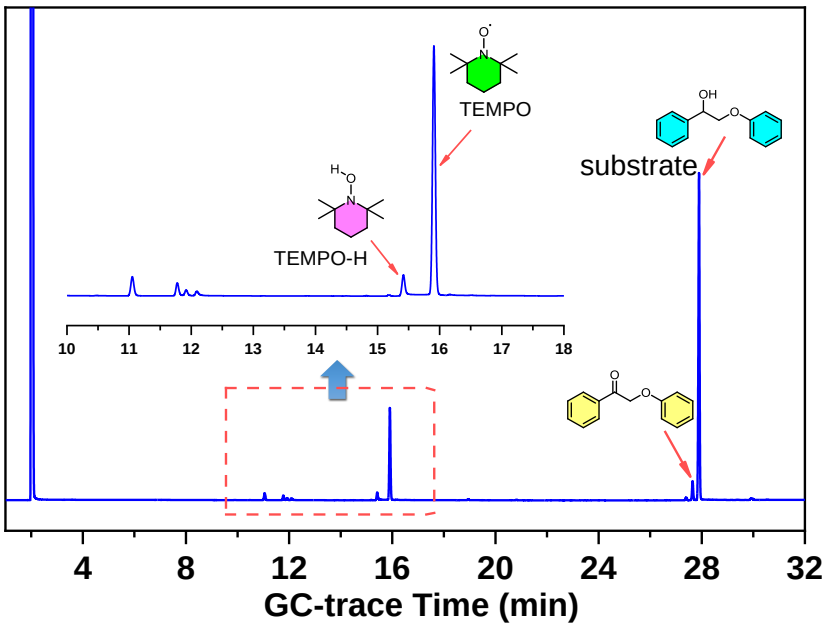

Figure S41. The GC-analysis for the inhibition impact of TEMPO on conversion of **6**. Reaction condition: 0.2 mmol of **6**, 5 mol% of PTP-dq·Cl and 30 mol% of TEMPO in 5 mL of acetonitrile in air at room temperature by irradiation with 365 nm light source for 180 min. GC heating method: The chromatographic column maintains a constant temperature of 80 ℃ for 8 minutes at the beginning. Subsequently, the temperature increases by 10 degrees Celsius per minute to 270 ℃. Lastly, the temperature lasts for 10 min.

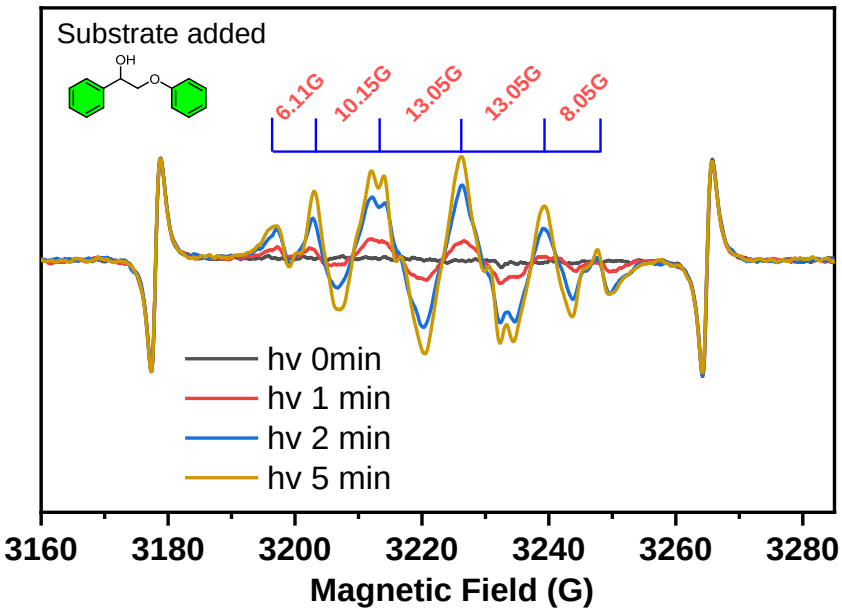

Figure S42. ESR spectra for the mixture of catalyst PTP-dq·Cl, 2-phenoxy-1-phenylethan-1-ol (1 mg) and DMPO (4 μL) in 1 mL of acetonitrile, irradiation with 365 nm light source under air at room temperature. The signals of the Mn (II) ion as internal standard are shown on the two sides for comparison.

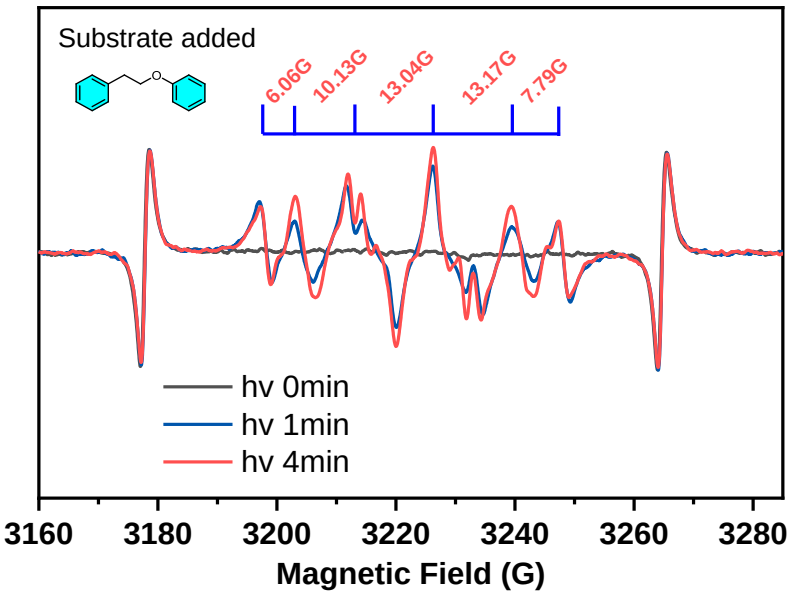

Figure S43. ESR spectra for the mixture of catalyst PTP-dq·Cl, 2-phenylethyl phenyl ether (1 mg) and DMPO (4 μL) in 1 mL of acetonitrile, irradiation with 365 nm light source under air at room temperature. The signals of the Mn (II) ion as internal standard are shown on the two sides for comparison.